Check for updates

the plant journal

SEB SOCIETY FOR EXPERIMENTAL BIOLOGY

The Plant Journal (2023) doi: 10.1111/tpj.16597

Arabidopsis BBX14 is involved in high light acclimation and seedling development

Vasil Atanasov[1], Julia Schumacher[2], Jose M. Muiño[2], Catharina Larasati[1], Liangsheng Wang[1,†], Kerstin Kaufmann[2], Dario Leister[1] and Tatjana Kleine[1,*]

[1]*Plant Molecular Biology (Botany), Department Biology I, Ludwig-Maximilians-University München, 82152 Martinsried, Germany,*

[2]*Chair for Plant Cell and Molecular Biology, Institute of Biology, Humboldt-Universität zu Berlin, Berlin, Germany*

Received 15 July 2023; revised 22 November 2023; accepted 1 December 2023.
*For correspondence (e-mail tatjana.kleine@lmu.de).
[†]Present address: State Key Laboratory of Plant Environmental Resilience, College of Biological Sciences, China Agricultural University, Beijing 100193, China

SUMMARY

The development of photosynthetically competent seedlings requires both light and retrograde biogenic signaling pathways. The transcription factor GLK1 functions at the interface between these pathways and receives input from the biogenic signal integrator GUN1. BBX14 was previously identified, together with GLK1, in a core module that mediates the response to high light (HL) levels and biogenic signals, which was studied by using inhibitors of chloroplast development. Our chromatin immunoprecipitation-Seq experiments revealed that *BBX14* is a direct target of GLK1, and RNA-Seq analysis suggests that BBX14 may function as a regulator of the circadian clock. In addition, BBX14 plays a role in chlorophyll biosynthesis during early onset of light. Knockout of *BBX14* results in a long hypocotyl phenotype dependent on a retrograde signal. Furthermore, the expression of *BBX14* and *BBX15* during biogenic signaling requires GUN1. Investigation of the role of BBX14 and BBX15 in GUN-type biogenic (*gun*) signaling showed that the overexpression of BBX14 or BBX15 caused de-repression of *CA1* mRNA levels, when seedlings were grown on norflurazon. Notably, transcripts of the *LHCB1.2* marker are not de-repressed. Furthermore, BBX14 is required to acclimate plants to HL stress. We propose that BBX14 is an integrator of biogenic signals and that BBX14 is a nuclear target of retrograde signals downstream of the GUN1/GLK1 module. However, we do not classify BBX14 or BBX15 overexpressors as *gun* mutants based on a critical evaluation of our results and those reported in the literature. Finally, we discuss a classification system necessary for the declaration of new *gun* mutants.

Keywords: acclimation, *Arabidopsis thaliana*, BBX14, GLK1, GUN1, retrograde signaling, seedling development.

INTRODUCTION

Light is indispensable for plants. Apart from driving photosynthesis, it is required to direct growth, as well as developmental and acclimation processes. For example, in darkness, etiolated/skotomorphogenic Arabidopsis seedlings develop long hypocotyls, unexpanded, and appressed cotyledons with etioplasts, and an apical hook that protects the apical meristem from damage (Han et al., 2020). On the other hand, photomorphogenetically de-etiolated seedlings change their form by inhibiting hypocotyl elongation, unfolding the hook, stimulating cotyledon separation and expansion, and activating the formation of fully functional chloroplasts (Von Arnim & Deng, 1996). At the heart of the light-dependent signal transduction network that controls this transition is the E3 ubiquitin ligase CONSTITUTIVE PHOTOMORPHOGENIC 1 (COP1). COP1 integrates signals from photoreceptors and regulates a set of downstream components including the transcription factors (TFs) ELONGATED HYPOCOTYL 5 (HY5) (Han et al., 2020; Podolec & Ulm, 2018), GOLDEN2-LIKE 1 (GLK1) and GLK2, which regulate genes involved in chlorophyll biosynthesis and formation of the photosynthetic apparatus (Waters et al., 2009), and B-box (BBX) proteins (Xu, 2020).

In plants, BBX proteins form a subgroup of zinc-finger TFs (Talar & Kielbowicz-Matuk, 2021), which is comprised of 32 members in *Arabidopsis thaliana* (Khanna et al., 2009). The B-box itself can mediate a variety of functions including protein–protein interactions (Datta et al., 2006) and activation

© 2023 The Authors.
The Plant Journal published by Society for Experimental Biology and John Wiley & Sons Ltd.
This is an open access article under the terms of the Creative Commons Attribution License, which permits use, distribution and reproduction in any medium, provided the original work is properly cited.

of transcription (Datta et al., 2007). The first BBX protein identified in Arabidopsis was CONSTANS (CO, BBX1), which promotes flowering (Putterill et al., 1995). In subsequent studies, very different names were used for members of the B-box family, which prompted Khanna et al. (2009) to propose a uniform nomenclature for them. These authors numbered them from BBX1 to BBX32, and sorted them into clades I to V, based on multiple sequence alignment, phylogenetic analysis, and the presence of additional domains. Clades I (BBX1–BBX6) and II (BBX7–BBX13) are characterized by two B-boxes and a CCT (CO, CO-LIKE, and TOC1) domain, and clade III (BBX14–BBX17) by a single B-box and a CCT domain, while members of clade IV (BBX18–BBX25) have two B-boxes, and those of clade V (BBX26-BBX32) have one. It is now known that BBX proteins participate in the regulation of plant growth and development, hormonal pathways, and biotic and abiotic stress tolerance (Gangappa & Botto, 2014; Khanna et al., 2009; Talar & Kielbowicz-Matuk, 2021; Vaishak et al., 2019; Xu, 2020). Moreover, different members of the group can act antagonistically, serving as positive and negative regulators of the same processes. For example, during seedling photomorphogenesis, BBX4 and BBX20–BBX23 (Datta et al., 2006, 2007, 2008; Fan et al., 2012; Zhang et al., 2017) have been identified as positive, and BBX18, BBX19, and BBX24, BBX25, and BBX28–BBX32 (Cao et al., 2022; Heng et al., 2019; Holtan et al., 2011; Khanna et al., 2006; Kumagai et al., 2008) as negative regulators, respectively.

The development of photosynthetically competent seedlings is strictly dependent on the exchange of information between plastids and the nucleus. Since most chloroplast proteins are encoded in the nucleus, it exercises anterograde control over the plastids (Jan et al., 2022). Conversely, during retrograde signaling, chloroplasts emit signals that convey information relating to their status to the nucleus, so that nuclear gene expression can be adjusted accordingly (Jan et al., 2022; Kleine & Leister, 2016; Liebers et al., 2022). This mechanism is exemplified by the response of seedlings to treatment with norflurazon (NF, an inhibitor of carotenoid biosynthesis) or inhibitors of organellar protein synthesis such as lincomycin (LIN): each of these agents reduces levels of transcripts derived from so-called photosynthesis-associated nuclear genes (*PhANG*s) (Oelmuller et al., 1986). Although the quest for *genomes uncoupled* (*gun*) mutants (i.e., seedlings that continue to express *PhANG*s even though plastid development has been blocked by NF or LIN) began 30 years ago, the mechanisms underlying this phenotype have yet to be fully clarified, and the number of known bona fide *gun* mutants now stands at less than 10 (Richter et al., 2023).

BBX14 (COL6), a member of clade III, attracted our attention because it was found together with GLK1 and GLK2 in a core module required for the nuclear retrograde response to altered organellar gene expression (Leister & Kleine, 2016). The identification of this module was based on database analyses, which indicated that changes in gene expression comparable to those provoked by treatment with LIN, NF, or high light (HL) also take place in two mutants that are defective in plastid gene expression. Using this module, overexpressors of GLK1 and GLK2 were shown to be *gun* mutants under both NF and LIN conditions (Leister & Kleine, 2016). Moreover, based on a co-expression network, BBX14 was suggested as a potentially important regulator of the response to HL levels (Huang et al., 2019).

The present study was designed to gain further insight into the function of BBX14. We identified *BBX14* as a direct target of GLK1, and RNA-Seq analysis of *bbx14* mutant seedlings reveals specific de-regulation of transcripts encoding proteins involved in the circadian clock. Lack of BBX14 compromises acclimation of plants to HL. Furthermore, BBX14 promotes seedling development, and the long hypocotyl phenotype seen in *bbx14* is comparable to that of one of the *glk1* mutant. This phenotype in turn depends on a retrograde signal, and reduction of *BBX14* and *BBX15* mRNA levels during biogenic signaling depends on GUN1. Transcript levels of several, but not all of the *PhANG* genes investigated are de-repressed in BBX14 overexpressors under NF treatment. However, a critical evaluation of our results and those reported in the literature led us to refrain from categorizing BBX14 overexpressors as *gun* mutants.

RESULTS

The *BBX14* gene is a direct target of GLK1

Levels of *BBX14*, *BBX15*, and *BBX27* transcripts are elevated in oeGLK1 and oeGLK2 lines (Waters et al., 2009), which suggests that these genes are targets of GLKs. To clarify whether or not *BBX14* is a direct target of GLK1, we performed a chromatin immunoprecipitation experiment, followed by sequencing (ChIP-seq), on 14-day-old seedlings of a plant line that expresses GLK1 from its endogenous promoter in the Col-0 background. Our ChIP-seq experiment confirmed binding of GLK1 to the *BBX16* promoter (Veciana et al., 2022) and detected a GLK1-bound genomic region directly upstream of the *BBX14* transcription start site (TSS). Analysis of this region revealed the presence of four GLK1 binding sites (Figure 1a), all of which match the CCAATC consensus identified in a set of co-expressed, photosynthesis-related genes (Kobayashi et al., 2012). One of these motifs, located 70 bp upstream of the TSS, could be further extended to yield a sequence that matches a GLK1-binding motif identified by protein-binding microarrays (*GATTCT*GATTGG; Franco-Zorrilla et al., 2014) and thus represents a strong candidate for GLK1 binding. This result indicates that *BBX14* is indeed a direct target of GLK1, and additional *BBX* genes were

© 2023 The Authors.

1365313x, 0, Downloaded from https://onlinelibrary.wiley.com/doi/10.1111/tpj.16597 by Cochrane Germany, Wiley Online Library on [08/03/2024]. See the Terms and Conditions (https://onlinelibrary.wiley.com/terms-and-conditions) on Wiley Online Library for rules of use; OA articles are governed by the applicable Creative Commons License

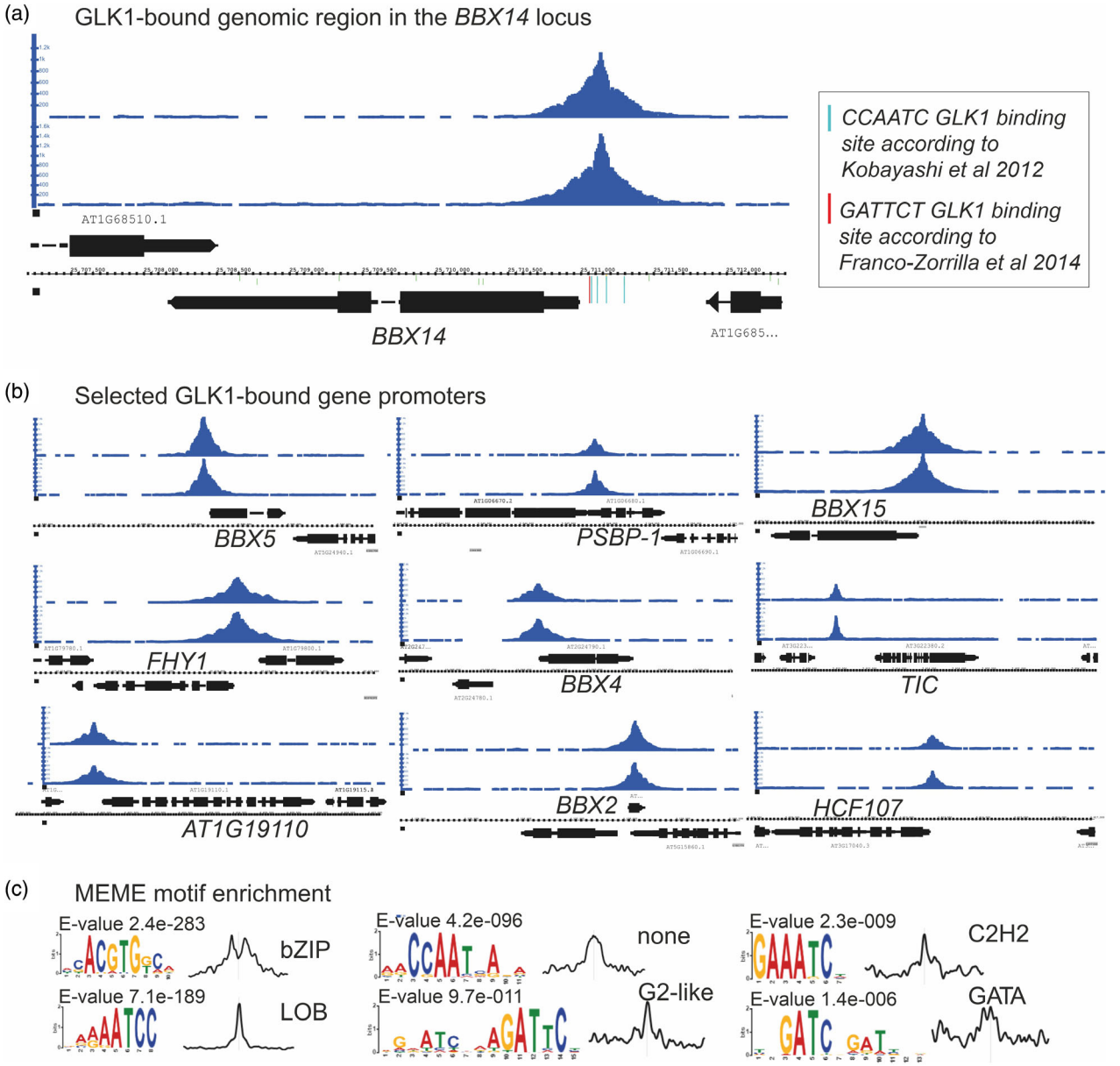

Figure 1. *BBX14* is a target of GLK1.
(a) Chromatin immunoprecipitation followed by sequencing (ChIP-seq) was performed with 14-day-old seedlings of a plant line that expresses GLK1 from its endogenous promoter in the Col-0 background (*pGLK1:GLK1-GFP*), and a snapshot of the *BBX14* gene region is shown.
(b) Snapshots of selected genes targeted by GLK1.
(c) Additional motifs bound by GLK1 identified by the MEME Suite (Bailey et al., 2015).

detected among the top 10 most highly enriched potential target genes (Table S1; Figure 1b). Furthermore, *TIME FOR COFFEE* (*TIC*), a component of the circadian clock, was among the top targets. Besides a motif that was identified as "G2-like" but resembles a GLK1 binding consensus, MEME-identified motifs resembling bZIP, LOB, C2H2, and GATA TF binding motifs as markedly enriched in the GLK1-bound genomic regions (Figure 1c), a finding that implies coordinated control of target gene activities. In fact, the *BBX14* core promoter is bound by GLK1 in combination with other TFs involved in light/circadian and cytokinin signaling, such as PIF4, LUX, HY5, PRR5, and ARR10 based on the ChIP-hub platform (Fu et al., 2022).

BBX14 plays a role in chlorophyll biosynthesis during early onset of light

BBX proteins have already been recognized as prominent factors in seedling development (see "Introduction" section),

© 2023 The Authors.

1365313x, 0, Downloaded from https://onlinelibrary.wiley.com/doi/10.1111/tpj.16597 by Cochrane Germany, Wiley Online Library on [08/03/2024]. See the Terms and Conditions (https://onlinelibrary.wiley.com/terms-and-conditions) on Wiley Online Library for rules of use; OA articles are governed by the applicable Creative Commons License

and GLKs are required for chlorophyll accumulation (Waters et al., 2009). To test for an abnormal seedling phenotype when BBX14 is absent, the mutant *bbx14-1* (SAIL_1221_D02) was identified in the SIGnAL database (Alonso et al., 2003; Figure S1a,b), and found to express *BBX14* transcripts in amounts equivalent to 10% of Col-0 levels (Figure S1c). Because *bbx14-1* was the sole T-DNA mutant line available, two independent CRISPR/Cas-mediated lines (*bbx14-2* and *bbx14-3*) were also generated. In *bbx14-2*, an insertion after nucleotide (nt) 924 relative to the start codon introduced a premature stop, and in *bbx14-3* a T-to-G change at nt 925 resulted in the replacement of a Trp by a Gly residue. In *bbx14-2*, *BBX14* transcript levels were reduced to 10% and in *bbx14-3*, interestingly, transcript levels were also reduced (to 25%) compared with Col-0 (Figure S1c). The involvement of BBX14 in seedling development is attested by observation of chlorophyll contents of seedlings grown for 3 days in darkness and then transferred into continuous light for 2, 4, and 8 h. GUN4 stimulates chlorophyll biosynthesis (Peter & Grimm, 2009), and therefore the *gun4-2* mutant, used as a control, showed reduced chlorophyll levels throughout the time course compared with Col-0 (Figure 2a). In *bbx14* mutant seedlings, chlorophyll accumulation was significantly reduced when transferred to light for 2 and 4 h. After 8 h, chlorophyll levels were similar to wild type (WT), indicating that BBX14 plays a major role in chlorophyll accumulation during early light onset.

BBX14 participates in the regulation of genes associated with the circadian clock

To gain insight into the molecular function of BBX14, we looked for transcriptome changes, focusing on light-independent and dependent or common targets. To this end, RNAs isolated from 3-day-old etiolated WT and *bbx14-1* seedlings and from 3-day-old etiolated seedlings exposed to 16 h of light and then 8 h of darkness again, were subjected to RNA sequencing (RNA-Seq).

In dark-grown *bbx14-1* seedlings, only four protein-coding transcripts were reduced (*ACTIN-RELATED PROTEIN 9* [*ARP9*], *ARABIDOPSIS RESPONSE REGULATOR 7* [*ARR7*], *MEMBRANE-ANCHORED UBIQUITIN-FOLD PROTEIN 5 PRECURSOR* [*MUB5*] and *AT5G26270*), and two elevated (*QUA-QUINE STARCH* [*QQS*] and *AT3G29633*) relative to WT (>2-fold, $P < 0.05$; Figure 2c,d; Table S2).

In the *bbx14-1* seedlings that had been exposed to 16 h light and then 8 h darkness, 147 protein-coding transcripts changed significantly relative to WT (>2-fold, $P < 0.5$; Table S3), of which 63 were reduced and 84 were elevated (Figure 2c,d). Three of them were among those whose expression was altered in the same sense as in etiolated *bbx14* seedlings and therefore represent light-independent targets of BBX14. Moreover, transcript levels of the clade II members *BBX7* and *BBX8* were reduced. In addition, lower levels of *PHOTOPERIODIC CONTROL OF*

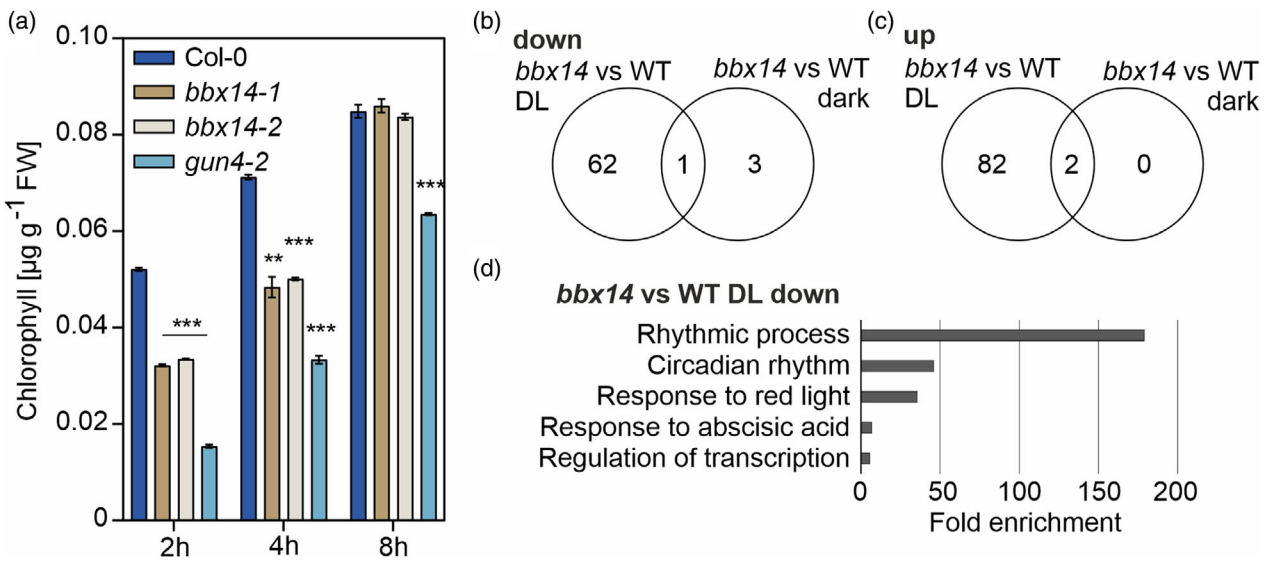

Figure 2. BBX14 is involved in seedling development.
(a) Determination of total chlorophyll (Chl *a* + *b*) content of seedlings grown in darkness and then transferred to light for the indicated time. Chlorophyll was acetone-extracted and measured spectrophotometrically, and concentrations were determined as described (see "Experimental procedures" section). Data are shown as mean values ± SD from three different plant pools. Each pool contained more than 100 seedlings.
(b, c) Analysis of transcriptome changes in *bbx14* mutant seedlings. Venn diagrams depicting the degree of overlap between the sets of genes whose expression levels were reduced (b) or elevated (c) by at least twofold in *bbx14-1* seedlings that had been exposed to LD (16 h light, 8 h dark) conditions or were grown in darkness compared with the respective WT (Col-0) control.
(d) Gene ontology (GO) analysis of genes whose expression is down-regulated in light-shifted *bbx14-1* seedlings. GO annotations for the biological process category were extracted from DAVID.

© 2023 The Authors.

1365313x, 0, Downloaded from https://onlinelibrary.wiley.com/doi/10.1111/tpj.16597 by Cochrane Germany, Wiley Online Library on [08/03/2024]. See the Terms and Conditions (https://onlinelibrary.wiley.com/terms-and-conditions) on Wiley Online Library for rules of use; OA articles are governed by the applicable Creative Commons License

HYPOCOTYL 1 (*PCH1*) and higher levels of *XYLOGLUCAN ENDOTRANSGLUCOSYLASE/HYDROLASE 9* (*XTH9*) and *XTH16* transcripts were detected. XTHs encode proteins involved in the weakening of cell–cell contacts and rearrangement of the cell wall. Gene ontology (GO) analysis with DAVID (Sherman et al., 2022) identified the GO "rhythmic process" as striking 180-fold enriched in the set of genes with reduced transcript levels (Figure 2d), represented for example by genes encoding the flavin-binding kelch-repeat F-box protein FKF1, PSEUDO-RESPONSE REGULATOR 5 (PRR5) and the CCT motif-containing response regulator protein TIMING OF CAB EXPRESSION 1 (TOC1). These findings might suggest a role for BBX14 as a regulator of the circadian clock, as has already been shown for BBX19 (Yuan et al., 2021). The binding of circadian clock-associated TFs to the *BBX14* promoter suggests the presence of feedback regulatory mechanisms, but here it has to be noted that, although *BBX14* expression is diurnally regulated, it was not detected as a strongly rhythmically active gene by the Arabidopsis eFP Browser (Winter et al., 2007). It is noteworthy that the expected target transcripts of GLKs, such as those encoding photosynthetic proteins or enzymes involved in chlorophyll biosynthesis (Waters et al., 2009), were not identified.

The *bbx14* mutant exhibits a long hypocotyl phenotype that depends on a retrograde signal

Since *BBX14* is a target of GLK1, we further investigated the correlation between BBX14 and GLK1. Levels of *BBX14* mRNA are dependent on GLK1 in light-grown *glk1* seedlings (Figure 3a) confirming a previous finding (Veciana et al., 2022), and *glk1* seedlings develop longer hypocotyls in the light. Accordingly, we found that hypocotyl lengths of *bbx14* and *glk1* mutants were likewise elongated (Figure 3b,c).

In germinating seedlings, chloroplast biogenesis is highly sensitive to environmental changes and requires "biogenic control" (Pogson et al., 2008), that is, signaling from chloroplasts to the nucleus during early developmental stages in which a GLK1-GUN1 module is involved (Leister & Kleine, 2016; Martin et al., 2016). When WT seedlings are grown under very low levels of white light (1 μmol m^{-2} sec^{-1}), LIN partially prevents de-etiolation, and hypocotyls are longer than those of seedlings grown in its absence (Martin et al., 2016). Because *bbx14* seedlings displayed a longer hypocotyl phenotype under our light intensity (100 μmol m^{-2} sec^{-1}) – a condition which serves as a test for *gun* phenotypes – we assessed hypocotyl growth in WT, *bbx14*, and *glk1* lines in the presence of LIN. Under our lighting conditions, hypocotyl lengths of WT seedlings were even shorter when grown on medium with LIN supplementation (Figure 3c), indicating that the etiolation phenotype in the presence of LIN is mainly observed under very low light levels. This is compatible with the fact that, when 2-day-old etiolated seedlings were transferred to white light levels of 25 μmol m^{-2} sec^{-1}, the same hypocotyl lengths were observed in the absence and presence of LIN (Martin et al., 2016). Strikingly, the long hypocotyl phenotype of *bbx14* and *glk1* seedlings was alleviated when seedlings were grown on LIN, and hypocotyl lengths were comparable to those of the WT (Figure 3c). This effect is not simply due to an energy shortage, because sugar provision did not revert the effect of LIN (Figure 3d), which suggests that the *bbx14* and *glk1* hypocotyl phenotypes are dependent on a retrograde signal. It was previously shown that the retrograde signaling and phytochrome pathways antagonistically regulate the phytochrome-interacting factors (PIF)-repressed transcriptional network (Martin et al., 2016), and the core promoter of *BBX14* is bound by PIF4 in addition to GLK1. Notably, *BBX14* mRNA levels were de-repressed in dark-grown *pifq* seedlings, which lack PIF1, -3, -4, and -5, and lincomycin treatment prevented this de-repression (Figure 3e).

Reduction of *BBX14* mRNA levels during biogenic signaling is dependent on GUN1

Data extracted from Genevestigator (https://genevestigator.com) suggested that, of the *BBX* members represented on the Affymetrix ATH1 chip (seven of the 32 *BBX* genes were not evaluated because they are not represented on the Affymetrix ATH1 genome array), levels of *BBX3*, *BBX14*, *BBX16*, and *BBX27* mRNAs are reduced in NF-treated seedlings, while under LIN conditions only *BBX14* and *BBX16* mRNAs are partially repressed (Figure 4a). As a complement to Genevestigator results, previously published RNA-Seq data (Habermann et al., 2020; Richter et al., 2020; Xu et al., 2020) were re-analyzed and the read depths of *BBX14* and *BBX16* transcripts were calculated with their TPM (Transcripts Per Kilobase Million) values (Figure 4b). As controls, read depths of *LIGHT HARVESTING CHLOROPHYLL A/B-BINDING PROTEIN 1.2* (*LHCB1.2*) and *BBX8* were calculated. *LHCB1.2* mRNA levels are known to be strongly reduced under NF or LIN treatment (Oelmuller et al., 1986), and *BBX8* was used as an example of other BBX members whose RNA levels were suggested not to be reduced under LIN or NF treatment. All investigated loci behaved as expected and confirmed the Genevestigator data (Figure 4b). Moreover, these data suggested that the decrease in *BBX14* and *BBX16* mRNA levels under NF conditions is alleviated in *gun1* and *gun5* mutants. BBX16 has previously been implicated in retrograde signaling (Veciana et al., 2022), and we suspected that BBX14 might also be a component of the GUN1-GLK1 module. The *gun1* mutant is special in that – unlike all the other *gun* mutants – it also shows the *gun* phenotype under LIN conditions (summarized in Richter et al., 2023). To find out whether LIN-mediated repression of *BBX14* is also dependent on GUN1, *BBX14* mRNA expression was evaluated in 4-day-

© 2023 The Authors.

1365313x, 0, Downloaded from https://onlinelibrary.wiley.com/doi/10.1111/tpj.16597 by Cochrane Germany, Wiley Online Library on [08/03/2024]. See the Terms and Conditions (https://onlinelibrary.wiley.com/terms-and-conditions) on Wiley Online Library for rules of use; OA articles are governed by the applicable Creative Commons License

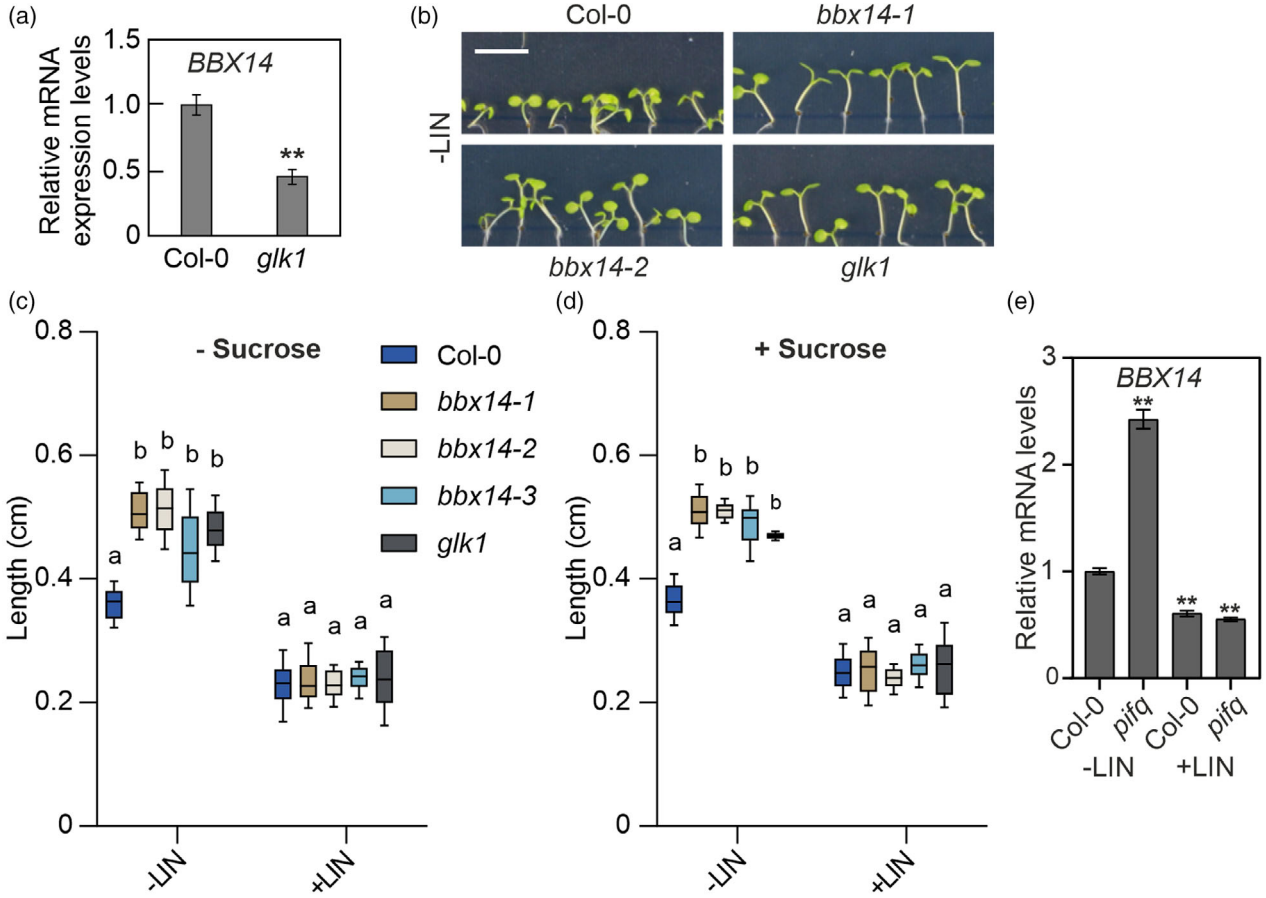

Figure 3. *BBX14* mutant exhibits a long hypocotyl phenotype that depends on a retrograde signal.
(a) *BBX14* mRNA levels in 3-day-old Col-0 and *glk1* mutant seedlings grown for 3 days under standard growth conditions (16-h light/8-h dark; 100 μmol photons m^{-2} sec^{-1}) as determined by RT-qPCR. The results were normalized to *AT4G36800*, which encodes a RUB1-conjugating enzyme (RCE1). Expression levels are reported relative to the corresponding transcript levels in Col-0 which were set to 1. Mean values ± SE were derived from three independent experiments, each with three technical replicates. Statistically significant differences (Tukey's test; $^{**}P < 0.01$) between wild-type (Col-0) and the *glk1* mutant are indicated.
(b) Phenotypes of Col-0 and mutant (*bbx14-1, bbx14-2, and glk1*) seedlings grown for 6 days under standard growth conditions without lincomycin (−LIN) supplementation. Scale bar = 0.5 cm.
(c) Quantification of hypocotyl lengths of Col-0 and mutant (*bbx14-1, bbx14-2, bbx14-3, and glk1*) seedlings grown for 6 days under standard growth conditions on MS medium without (−LIN), or with inhibitor supplementation (+LIN). The center line of boxplots indicates the median, the box defines the interquartile range, and the whiskers indicate minimum and maximum values from three independent experiments, each containing at least 50 seedlings. Statistically significant differences between the wild type and each mutant line under every condition are highlighted by letters above the plots (two-way ANOVA; a, no significant difference; b, $P < 0.0002$).
(d) Quantification of hypocotyl lengths of seedlings grown under the same conditions as in (C), but with addition of sucrose (1%) to the growth medium.
(e) RT-qPCR of *BBX14* mRNA levels in 3-day-old dark-grown Col-0 and *pifq* seedlings in the absence (−LIN) or presence of lincomycin (+LIN). RT-qPCR was performed as described in (A). Expression values are reported relative to the corresponding transcript levels in Col-0 grown without LIN, which were set to 1.

old Col-0 and *gun1-102* seedlings grown on Murashige and Skoog (MS) in the absence or presence of LIN. Under LIN treatment *BBX14* levels were reduced to 17% in Col-0 compared to control conditions (Figure 4c), and this effect was dependent on GUN1 since *BBX14* expression recovered almost completely in *gun1-102* seedlings treated with LIN. This, together with ChIP-Seq data (Figure 1) and the nuclear localization of BBX14 (Figure 4d), suggests that BBX14 might act as a transducer for GUN1/GLK1-dependent retrograde signals in the nucleus.

Characterization of BBX14 overexpression seedlings

We hypothesized that, like oeGLK lines (Leister & Kleine, 2016; Martin et al., 2016), overexpression of BBX14 could result in a *gun* phenotype, or a lack of BBX14 could evoke a *LHCB1.2* hypersensitive phenotype. To create plants that overexpress BBX14 (oeBBX14), Col-0 plants were transformed with a DNA fragment comprised of the *35S* Cauliflower Mosaic Virus promoter and the coding sequence of *BBX14*, fused upstream of either the enhanced

© 2023 The Authors.

1365313x, 0, Downloaded from https://onlinelibrary.wiley.com/doi/10.1111/tpj.16597 by Cochrane Germany, Wiley Online Library on [08/03/2024]. See the Terms and Conditions (https://onlinelibrary.wiley.com/terms-and-conditions) on Wiley Online Library for rules of use; OA articles are governed by the applicable Creative Commons License

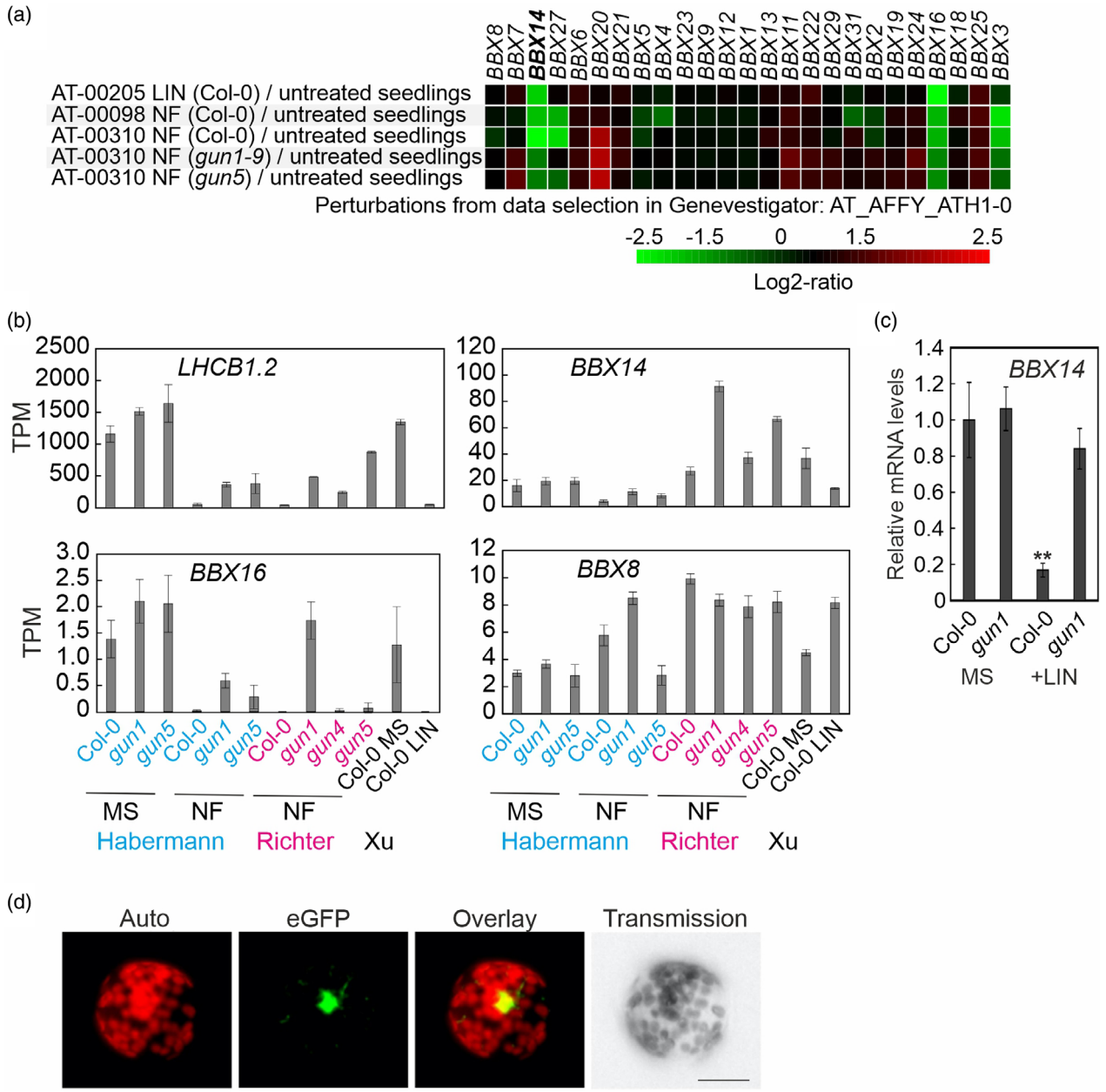

Figure 4. *BBX14* mRNA expression depends on retrograde signals.

(a) The reduction of *BBX14* mRNA levels during biogenic signaling depends on GUN1. Global profiling of *BBX* mRNA levels in response to perturbations were determined with Genevestigator, and studies involving lincomycin (LIN) and norflurazon (NF) treatments are shown. Note that seven out of the 32 *BBX* genes were not assessed due to their absence from the Affymetrix ATH1 genome array.

(b) TPM (transcripts per kilobase million) values of re-analyzed RNA-Seq data published by Habermann et al. (2020), Richter et al. (2020) and Xu et al. (2020).

(c) RT-qPCR of *BBX14* mRNA levels in Col-0 and *gun1* seedlings grown for 4 days in continuous light (100 μmol photons m^{-2} sec^{-1}) in the absence (MS) or presence of lincomycin (+LIN). Expression values are reported relative to the corresponding transcript levels in Col-0 grown on MS, which were set to 1. Mean values ± SE were derived from three independent experiments, each with three technical replicates. Statistically significant differences (Tukey's test; $^{**}P < 0.01$) between wild-type and mutant are indicated.

(d) BBX14 is localized to the nucleus. Fluorescence microscopy of tobacco protoplasts transiently expressing BBX14 fused to eGFP. The eGFP fluorescence (green) and chloroplast autofluorescence (red) are shown together in the overlay picture. Scale bar = 10 μm.

green fluorescence protein (eGFP) or a hemagglutinin (HA) tag. After selection for the resistance marker, 10 lines for each construct were identified, but fusion proteins were detected in only three of the oeBBX14-eGPF lines and two oeBBX14-HA lines (Figure 5a). Only one of these lines expressed higher levels (2.2-fold) of the *BBX14* transcript than Col-0 plants, while the others contained slightly less than the wild-type control (Figure 5b). Therefore, the

© 2023 The Authors.

1365313x, 0, Downloaded from https://onlinelibrary.wiley.com/doi/10.1111/tpj.16597 by Cochrane Germany, Wiley Online Library on [08/03/2024]. See the Terms and Conditions (https://onlinelibrary.wiley.com/terms-and-conditions) on Wiley Online Library for rules of use; OA articles are governed by the applicable Creative Commons License

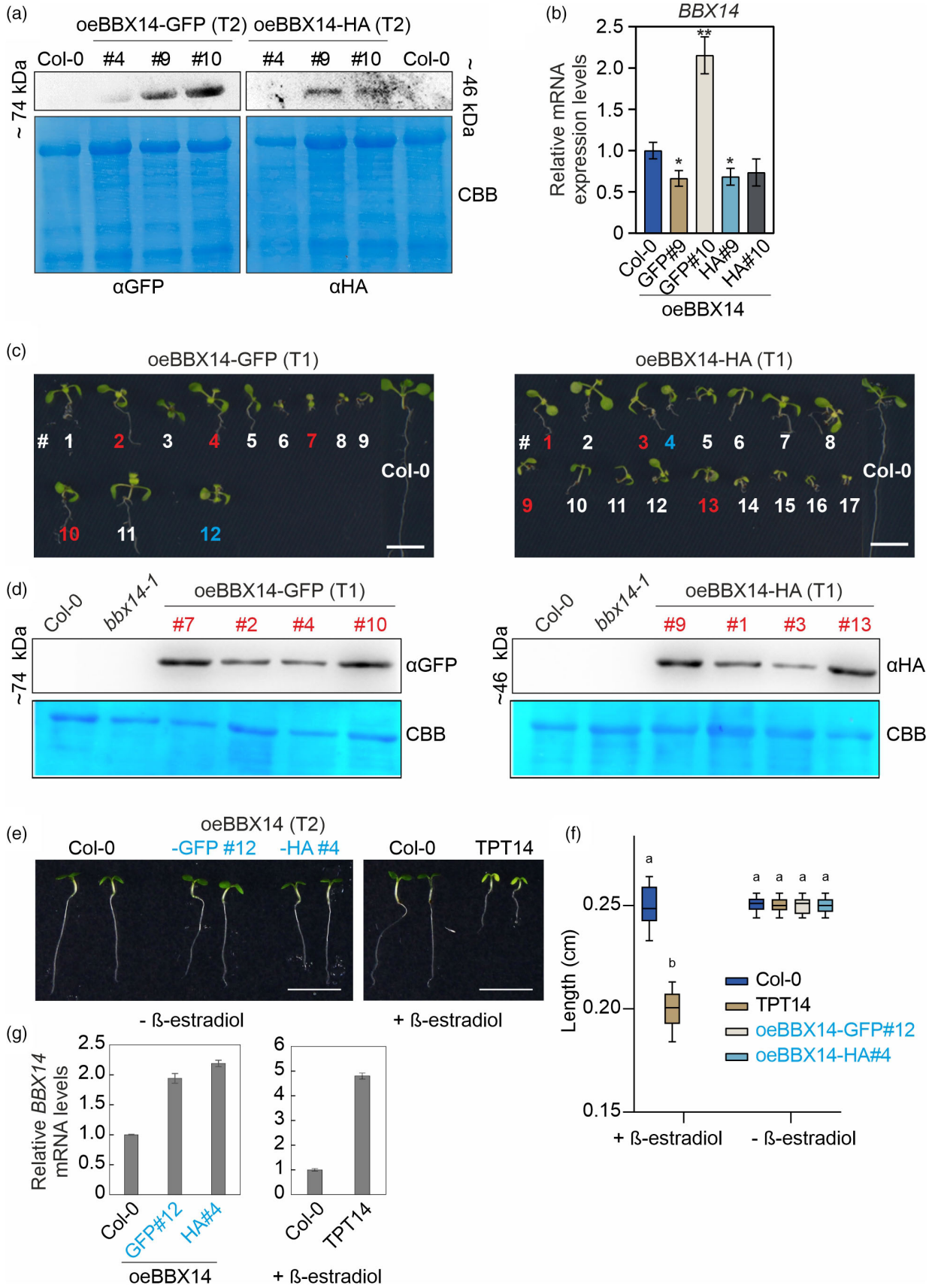

© 2023 The Authors.

1365313x, 0, Downloaded from https://onlinelibrary.wiley.com/doi/10.1111/tpj.16597 by Cochrane Germany, Wiley Online Library on [08/03/2024]. See the Terms and Conditions (https://onlinelibrary.wiley.com/terms-and-conditions) on Wiley Online Library for rules of use; OA articles are governed by the applicable Creative Commons License

Figure 5. Overexpression of *BBX14* may have detrimental effects.
(a) Total leaf proteins were isolated from 2-week-old Col-0 and Col-0 plants transformed with constructs containing *BBX14-eGFP* or *BBX14-HA* fusions, which were placed under the control of the *35S* promoter. Aliquots were fractionated by 10% SDS-PAGE gels under reducing conditions and subjected to immunoblotting using antibodies raised against the GFP- or HA-tag, respectively. PVDF membranes were stained with Coomassie brilliant blue (CBB) to control for protein loading. Representative blots from two experiments are presented. Relative sizes of the BBX14-GFP and BBX14-HA fusion proteins are indicated.
(b) RT-qPCR of *BBX14* mRNA expression in 7-day-old wild-type (Col-0), and in Col-0 plants "overexpressing" BBX14 (oeBBX14). RT-qPCR was performed as described in the legend to Figure 3(a).
(c) Phenotypes of 10-day-old wild-type (Col-0) seedlings, and Col-0 seedlings transformed with constructs containing the coding region of *BBX14* fused to either the GFP- (left panel) or the HA-tag (right panel), which were placed under the control of the *35S* promoter. Seedlings labeled in red provided the protein extracts from T1 plants that were subjected to SDS-PAGE in (d). The T2 generation of seedlings marked in turquoise was utilized to create images and data in (E, F), respectively. Scale bar = 0.5 cm.
(d) Aliquots of total leaf proteins were isolated from plants as indicated in (c), fractionated on SDS-PAGE gels (10%) under reducing conditions, and subjected to immunoblotting using antibodies raised against the GFP- or HA-tag, respectively. PVDF membranes were stained with Coomassie brilliant blue (CBB) to show protein loading.
(e) Phenotypes of 4-day-old Col-0 seedlings and the inducible BBX14 (TPT14) overexpression line grown under standard conditions (16-h light/8-h dark and 100 μmol photons m^{-2} sec^{-1}) in the absence (−β-estradiol) or presence of β-estradiol. Scale bars = 0.5 cm.
(f) Quantification of hypocotyl lengths of seedling grown as in (e). The center line of boxplots indicates the median, the box defines the interquartile range, and the whiskers indicate minimum and maximum values from three independent experiments, each containing at least 50 seedlings. Statistically significant differences between the wild type and each mutant line under every condition are highlighted by letters above the plots (two-way ANOVA; a, no significant difference; b, $P < 0.0002$).
(g) RT-qPCR of *BBX14* mRNA expression in seedlings shown in (e). RT-qPCR was performed as described in the legend to Figure 3(a).

remaining seeds of the Col-0 plants bearing the overexpression constructs were again subjected to selection, and all resistant seedlings were transferred to MS without herbicide. In this way, we selected lines based on a paler and smaller phenotype compared to Col-0 seedlings (Figure 5c). Western blot analysis indicated that the severity of the seedling phenotype might be related to the degree of BBX14 overexpression (Figure 5d). However, this phenotype was not observed in the T2 generation (Figure 5e). To further investigate this, we made use of an inducible BBX14 line (named TPT14; only one line available) generated within the TRANSPLANTA collection (Coego et al., 2014). After 4 days of induction, TPT14 seedlings were clearly perturbed (Figure 5e) and displayed shorter hypocotyls (Figure 5f), while they had a WT-like hypocotyl when not induced. Notably, a lack of BBX14 resulted in longer hypocotyls (Figure 3). Again, the hypocotyl phenotype may be attributed to the degree of BBX14 overexpression. In the T2 generation, the oeBBX14-tag lines only demonstrated a 2-fold elevation in *BBX14* transcript abundance compared with Col-0 plants. This is a similar level of *BBX14* overexpression as seen in previously published BBX14 overexpressors (Buelbuel et al., 2023). In contrast, BBX14 mRNA levels were increased 5-fold in the induced TPT14 plants (Figure 5g).

Involvement of BBX14 and BBX15 in GUN-mediated retrograde signaling?

To test an involvement of BBX14 in *gun* signaling, Col-0, *gun1-102* (as a control), the *bbx14* mutant and the strongest "overexpression" seedlings (oeBBX14-GFP#10) were grown in the presence or absence of LIN for 4 days under continuous light (100 μmol m^{-2} sec^{-1}). After LIN treatment, *gun1-102* showed, as expected, enhanced expression of *LHCB1.2* mRNA relative to WT seedlings, but *LHCB1.2* levels were unchanged in both *bbx14* mutants and the "oeBBX14" line (Figure S2a). Also, the expression of *LHCB2.1* and *LHCB2.4* was not affected in lines with altered *BBX14* levels (Figure S2b). However, slightly higher *CA1* levels were observed in "oeBBX14" (Figure S2b). It is reasonable to assume that a 2.2-fold induction of BBX14 (Figure 5b) is insufficient to cause a true *gun* phenotype, so we wanted to investigate the *gun* phenotype in the TPT14 line. In order to circumvent secondary effects (Figure 5e), we employed a different experimental set-up to test for *gun* phenotypes. Seedlings were first grown for 3 days in darkness in the absence or presence of inhibitor (NF or LIN), then sprayed with the inducer, put back in the dark for 2 h, transferred into the light for 16 h (100 μmol m^{-2} sec^{-1}), and then harvested for quantitative real-time PCR (qRT-PCR). Interestingly, *BBX14* induction was higher in seedlings treated with NF than in seedlings treated with LIN or grown without inhibitor (Figure 6a). In the absence of inhibitor, *RBCS1A* expression levels were similar to those seen in Col-0 in all lines tested, but *LHCB1.2* and *CA1* levels were slightly elevated in *gun1* and *TPT14* seedlings (Figure 6b). In addition, the suitability of this protocol for *gun* phenotype evaluation was confirmed by de-repression of the retrograde signaling marker genes *LHCB1.2*, *CARBONIC ANHYDRASE 1* (*CA1*) and *RIBULOSE BISPHOSPHATE CARBOXYLASE SMALL CHAIN 1A* (*RBCS1A*) in *gun1* seedlings (Figure 6b). In TPT14, *LHCB1.2* mRNA accumulation varied greatly between experiments and was only two-fold upregulated, if at all (Figure 6b), which is also exemplified by the expression ratio of *LHCB1.2* between NF and MS samples. However, in the presence of NF, the mRNA levels of *CARBONIC ANHYDRASE 1* (*CA1*) and *RIBULOSE BISPHOSPHATE CARBOXYLASE SMALL CHAIN 1A* (*RBCS1A*) were comparable to those found in the *gun1* mutant in the TPT14 line. To get a broader overview on putative targets regulated by BBX14 during the onset of retrograde signaling, RNAs isolated from Col-0, *gun1*, and TPT14 seedlings

© 2023 The Authors.

1365313x, 0, Downloaded from https://onlinelibrary.wiley.com/doi/10.1111/tpj.16597 by Cochrane Germany, Wiley Online Library on [08/03/2024]. See the Terms and Conditions (https://onlinelibrary.wiley.com/terms-and-conditions) on Wiley Online Library for rules of use; OA articles are governed by the applicable Creative Commons License

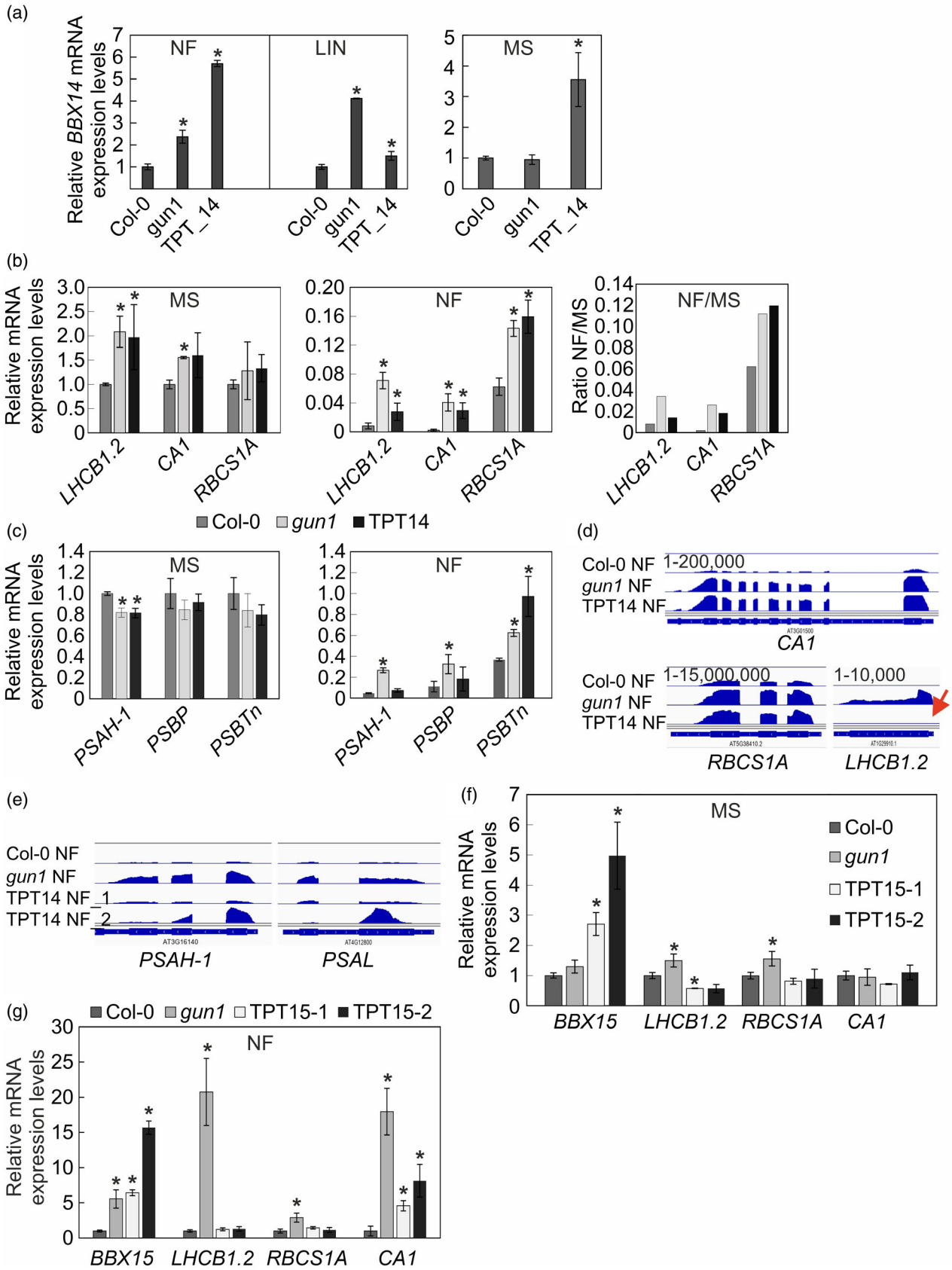

© 2023 The Authors.

1365313x, 0, Downloaded from https://onlinelibrary.wiley.com/doi/10.1111/tpj.16597 by Cochrane Germany, Wiley Online Library on [08/03/2024]. See the Terms and Conditions (https://onlinelibrary.wiley.com/terms-and-conditions) on Wiley Online Library for rules of use; OA articles are governed by the applicable Creative Commons License

Figure 6. Overexpression of BBX14 or BBX15 does not result in clear *gun* phenotypes.
(a) Levels of *BBX14* mRNAs in seedlings grown for 3 days in the dark in the presence of NF, LIN or no supplementation, sprayed with inducer, put back for 2 h in the dark, placed for 16 h into light (100 μmol m^{-2} sec^{-1}) and then harvested for qRT-PCR. The results were normalized to *RCE1*. Expression values are reported relative to the corresponding transcript levels in Col-0, which were set to 1. Mean values were derived from four independent experiments, each with three technical replicates. Bars indicate standard deviations. Statistically significant differences (Tukey's test; $P < 0.05$) between Col-0 and mutant samples are indicated by an asterisk.
(b) Transcript levels of the retrograde marker genes *LHCB1.2*, *CA1*, and *RBCS1A* (b), and *PHOTOSYSTEM I* (*PSI*) *SUBUNIT H-1* (*PSAH-1*), and *PSII SUBUNIT P* (*PSBP*) and *–Tn* (*PSBTn*) (c) in seedlings treated as in (a). Statistics were done as described in (a). NF/MS shows the expression ratio of seedlings grown on plates with NF versus those grown on plates without an inhibitor.
(d) Snapshots of RNA-Seq data. The read depths were visualized with the Integrative Genomics Viewer (IGV). The red arrow points out *LHCB1.2* expression, which is not increased in TPT14.
(e) Snapshots demonstrating the accumulation of the photosynthesis genes *PSAH-1* and *PSAL*.
(f, g) Transcript levels of *BBX15* and retrograde marker genes in Col-0, *gun1* and TPT15-1 and -2 seedlings treated as in (a) and grown on MS plates without inhibitor (f), or supplemented with NF (g). Statistics were done as described in (a).

grown on NF, and induced as described, were subjected to mRNA-Seq. Note here that only duplicates were used. In *gun1* seedlings, 901 and 1080 genes whose mRNA levels were more than two-fold (no adjusted *P*-value because of reasons explained in the methods part) reduced and elevated, respectively, relative to WT, and transcripts for Lhcb proteins were among the strongest up-regulated transcripts (Figure S3a; Table S4). The number of de-regulated transcripts in TPT14 was lower. However, 252 genes were identified whose transcripts were elevated in both *gun1* and TPT14 (Figure S3a). These included *RBCS1A* and *CA1*, confirming qRT-PCR results. Notably, GO analysis on this list identified "Photosynthesis" and "Cellular nitrogen compound biosynthesis" among the most highly enriched categories (Figure S3b). Because the RNA-Seq analysis was done without an adjusted *P*-value cutoff, another three of the identified targets were investigated by RT-qPCR. In the absence of inhibitor, *PHOTOSYSTEM I* (*PSI*) *SUBUNIT H-1* (*PSAH-1*), and *PSII SUBUNIT P* (*PSBP*) and *-Tn* (*PSBTn*) mRNA levels were comparable among all genotypes. In response to NF, the mRNA levels of all investigated transcripts were higher in the *gun1* mutant, but only *PSBT* was significantly elevated in the TPT14 line (Figure 6c). In addition, *LHCB1.2* was not identified as higher expressed in TPT14 after NF treatment (Table S4), consistent with the visualization of the expression pattern by plotting the read depths of the RNA-Seq data over *LHCB1.2* and as a control over the *CA1* and *RBCS1A* genes (Figure 6d). In addition, visualizing the accumulation of photosynthesis transcripts identified by enrichment analysis shown in Figure S3 resulted in an ambiguous picture (Figure 6e).

The clade III of BBX proteins comprises BBX14–BBX17. The consequence of overexpression of BBX16 on *gun* signaling was investigated before (Veciana et al., 2022). Moreover, *BBX15* is a direct target of GLK1 (Figure 1), therefore, also inducible BBX15 lines, TPT15-1 and -2, were tested. Induction of *BBX15* mRNA levels in the TPT15 lines was successful (Figure 6f), and the mRNA levels of retrograde marker genes were not changed under control conditions (Figure 6f). In response to NF, mRNA levels of *CARBONIC ANHYDRASE 1* (*CA1*) were elevated in both TPT15 lines (Figure 6g), but *RBCS1A* and *LHCB1.2* levels were comparable to levels found in the WT.

These results suggest that, like BBX16 (Veciana et al., 2022), BBX14 and BBX15 do not mediate regulation of *LCHB1.2* during retrograde signaling, but alter the expression of other *PhANG*s, such as *CA1* and *RBCS1A* (in the case of BBX14) or *CA1* (in the case of BBX15). However, we refrain from categorizing overexpressors of BBX14 or BBX15 as *gun* mutants (see "Discussion" section).

BBX14 is needed to acclimate plants to HL stress

Steady-state amounts of the *BBX14* transcript are reduced in plants exposed to HL levels (Garcia-Molina et al., 2020; Huang et al., 2019; Kleine et al., 2007; Leister & Kleine, 2016), as confirmed by the Genevestigator perturbations tool (https://genevestigator.com; Figure 7a). Interestingly, among all the *BBX* members represented on the Affymetrix ATH1 chip, this decrease in expression levels after HL treatment was quite specific for *BBX14*. In fact, Huang et al. (2019) identified *BBX14* as one of the top three hub genes in an HL co-expression network, suggesting that BBX14 may be an important regulator of the HL response. It could be expected that overexpression of BBX14 may support plants in tolerating HL, and here a two-fold increase in BBX14 levels may be sufficient. To gain insight into a putative function of BBX14 in the response to HL, 1-week-old Col-0, *bbx14-1*, *bbx14-2*, and "oeBBX14" plants grown under normal lighting conditions (80 μmol photons m^{-2} sec^{-1}) were exposed to a higher light level (1000 μmol photons m^{-2} sec^{-1}), which was sufficient to strongly reduce *BBX14* mRNA levels (Figure 7b). Importantly, for this experiment LED chambers were used that allowed for strict temperature control and eliminated the contribution of heat. Maximum quantum yield of PSII (F_v/F_m) was monitored under control conditions, after 3, 8, and 12 h of HL treatment, and thereafter recorded after 12 and 36 h of de-acclimation. Under standard light levels, 1-week-old *bbx14* and "oeBBX14" plants largely resembled the WT (Figure 7c; Figure S4). Under HL treatment, the "oeBBX14" plants behaved essentially as the WT (Figure S4). However, in *bbx14* mutant plants, a reduction

© 2023 The Authors.

1365313x, 0, Downloaded from https://onlinelibrary.wiley.com/doi/10.1111/tpj.16597 by Cochrane Germany, Wiley Online Library on [08/03/2024]. See the Terms and Conditions (https://onlinelibrary.wiley.com/terms-and-conditions) on Wiley Online Library for rules of use; OA articles are governed by the applicable Creative Commons License

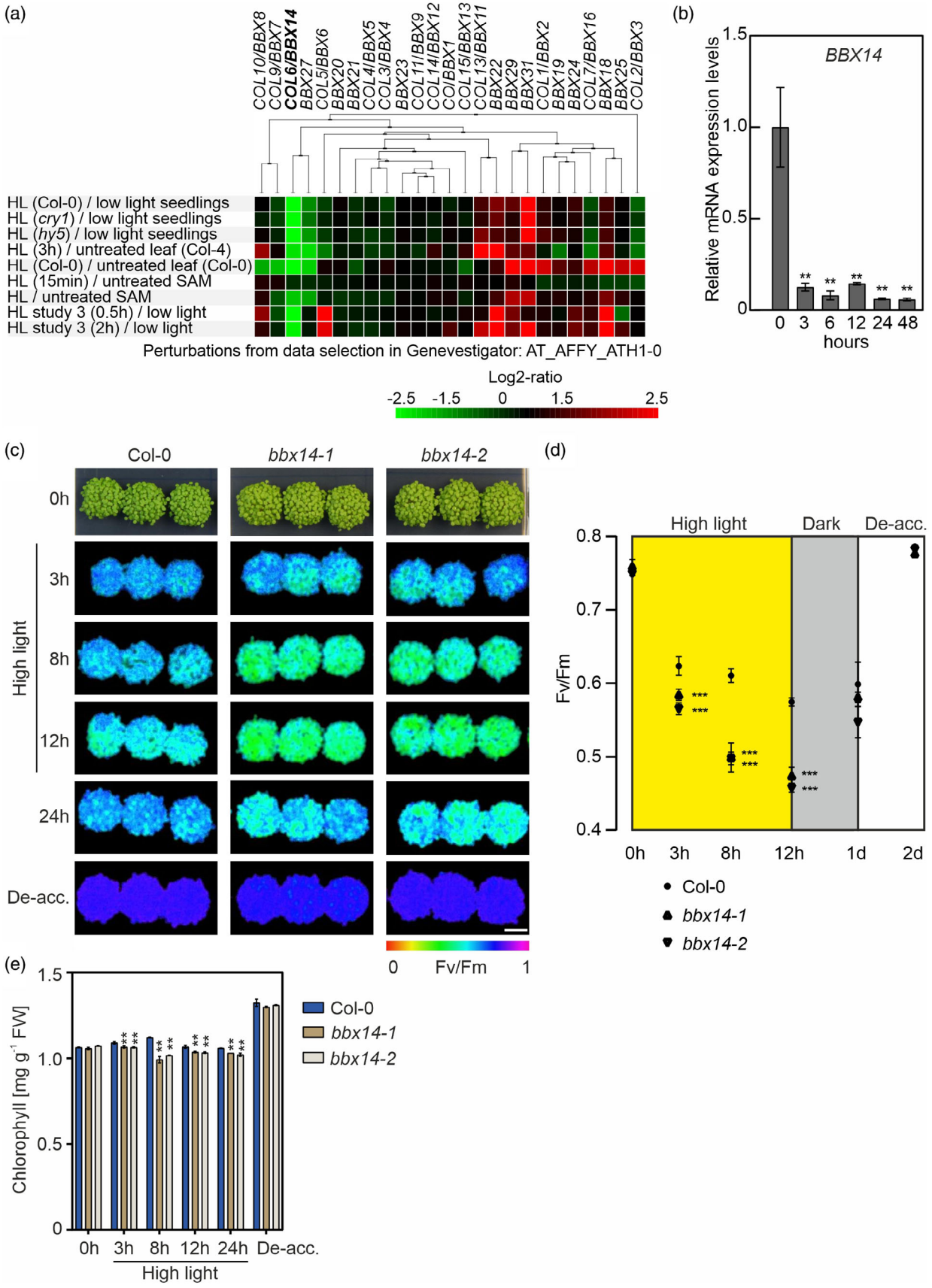

© 2023 The Authors.

1365313x, 0, Downloaded from https://onlinelibrary.wiley.com/doi/10.1111/tpj.16597 by Cochrane Germany, Wiley Online Library on [08/03/2024]. See the Terms and Conditions (https://onlinelibrary.wiley.com/terms-and-conditions) on Wiley Online Library for rules of use; OA articles are governed by the applicable Creative Commons License

Figure 7. BBX14 is involved in high light (HL) acclimation.
(a) Global profiling of *BBX* mRNA levels in response to perturbations was carried out with Genevestigator, and studies involving HL treatments are shown. The cladogram at the top summarizes the degree of relatedness between the expression profiles of the different *BBX* genes. SAM, shoot apical meristem.
(b) RT-qPCR of *BBX14* expression in 7-day-old Col-0 plants grown under control conditions and then shifted to light level for up to 2 days. The results were normalized to *AT4G36800*, which encodes a RUB1-conjugating enzyme (RCE1). Expression values are reported relative to the corresponding transcript levels in Col-0, which were set to 1. Mean values ± SE were derived from two independent experiments, each performed with three technical replicates per sample. Statistically significant differences (Tukey's test; $^{**}P < 0.01$) between control and each HL time point are indicated.
(c) Phenotypes and Imaging PAM pictures of Col-0 and mutant (*BBX14-1*, *BBX14-2*) plants grown for 1 week under control conditions (16-h light/8-h dark, 80 μmol photons m^{-2} sec^{-1}; left panel), shifted to HL conditions (16-h light/8-h dark, 1000 μmol photons m^{-2} sec^{-1}), and then de-acclimated (de-acc.) in control conditions. Scale bar = 1 cm.
(d) Photosystem II maximum quantum yield (F_v/F_m) of wild type (Col-0) and mutant (*BBX14-1 and BBX14-2*) seedlings grown as described in (c).
(e) Determination of total chlorophyll (Chl *a* + *b*) contents of seedlings grown as in (c). Data are shown as mean values ± SD from three different plant pools. Each pool contained more than 100 seedlings. Statistically significant differences (Tukey's test; $^{**}P < 0.01$) between control and each HL time point are indicated.

in F_v/F_m (relative to WT) was readily apparent after 3 h (Figure 7d) and was intensified throughout the HL time course. Nevertheless, *bbx14* plants could recover their F_v/F_m values after de-acclimation in normal growth conditions (Figure 7c,d). Furthermore, while the chlorophyll content of *bbx14* seedlings was similar to that of the WT under control conditions, it decreased slightly but significantly under HL treatment (Figure 7e). Notably, the *bbx14* HL phenotype was not due to reduced chlorophyll accumulation. The *gun4-2* mutant, used as a control, showed reduced chlorophyll levels compared with Col-0 (Figure S4). However, *gun4-2* plants displayed an even higher F_v/F_m value relative to WT throughout the HL time course (Figure S4). Overall, BBX14 is beneficial for plant growth under this HL set-up.

DISCUSSION

Emerging functions of BBX clade III members in seedling development

BBX proteins are vital for plant development and have also emerged as players in the process of acclimation to adverse environmental conditions (Alvarez-Fernandez et al., 2021; Talar & Kielbowicz-Matuk, 2021). Together with BBX15–BBX17, BBX14 belongs to clade III of the B-box proteins (Khanna et al., 2009). BBX16 was first described 10 years ago as a phytochrome-B-dependent regulator of branching and the shade avoidance response (Wang et al., 2013; Zhang et al., 2014). Meanwhile, more information has become available about the functions of the members of this clade. Thus, BBX17 was recently suggested to interact with CONSTANS to negatively regulate flowering time (Xu et al., 2022), and BBX14 was found to negatively regulate nitrogen starvation- and dark-induced senescence (Buelbuel et al., 2023). Additionally, BBX14/15/16 were identified as components of a GLK-BBX module that inhibits precocious flowering (Susila et al., 2023).

BBX16 has emerged as a promoter of seedling photomorphogenesis and as an element that acts downstream of the GUN1/GLK1 module during retrograde signaling (Veciana et al., 2022). Indeed, BBX14 first aroused our interest when we identified it in a core-response module for the HL and retrograde signaling response (Leister & Kleine, 2016) situated at the interface of seedling development, retrograde, and acclimation pathways. Studies of BBX proteins are hampered by functional redundancies. For example, the hypocotyls of the *bbx28 bbx29 bbx30 bbx31* quadruple mutant are shorter than those of double and single mutants (Song et al., 2020), which suggests that the clade V members BBX28, BBX29, BBX30, and BBX31 additively repress seedling photomorphogenesis (Song et al., 2020). Within clade III, BBX15 is most closely related to BBX14, followed by BBX16 and BBX17 (Khanna et al., 2009). While a loss of BBX14 results in a clear seedling phenotype (our results), the involvement of BBX14 in the regulation of flowering time was only revealed by the simultaneous knock-down of BBX14, -15, and -16 (Susila et al., 2023). Conversely, cotyledon phenotypes were more clearly revealed by overexpression of BBX16 than in *bbx16* mutant lines (Veciana et al., 2022).

In addition, feedback regulation further complicates the study of BBX proteins. For example, while *BBX30* and *BBX31* are transcriptionally repressed by HY5 (Heng et al., 2019), BBX28 and BBX29 act together to prevent HY5 from binding to the promoters of *BBX30* and *BBX31*, resulting in the expression of these genes. In addition, BBX30 and BBX31 interact with the promoters of *BBX28* and *BBX29* and enhance their expression (Song et al., 2020), and BBX29 undergoes COP1-mediated degradation in the dark (Heng et al., 2019). *BBX14-16* are all targets of GLK1, but it can be safely assumed that future research will reveal more complex modes of action for these proteins. Such studies will also clarify whether BBX15 affects seedling development and whether a *bbx14 bbx15 bbx16* triple mutant has a greater impact on plant development than any of the single or double mutant combinations.

Does the declaration of new "*gun*" mutants require a classification system?

The quest for *gun* mutants began 30 years ago, a screen designed to uncover components of the retrograde

© 2023 The Authors.

1365313x, 0, Downloaded from https://onlinelibrary.wiley.com/doi/10.1111/tpj.16597 by Cochrane Germany, Wiley Online Library on [08/03/2024]. See the Terms and Conditions (https://onlinelibrary.wiley.com/terms-and-conditions) on Wiley Online Library for rules of use; OA articles are governed by the applicable Creative Commons License

signaling pathway in seedlings led to the identification of the chloroplast-localized GENOMES UNCOUPLED (GUN) proteins (Susek et al., 1993). While all *gun* mutants de-repress *PhANG*s under NF treatment, *gun1* alone responds in the same manner in the presence of LIN (Koussevitzky et al., 2007). Especially recently several new "*gun*" mutants have been postulated, mostly based on subtle *PhANG* accumulation phenotypes, preferably detected by qPCR. However, we claim that the number of known bona fide *gun* mutants still stands at less than 10 (Richter et al., 2023). For example, among the quite recently identified new "*gun*" mutants in the GUN1 branch are overexpressors of MORF2 (Zhao et al., 2019). In this publication, qPCR was used to detect 3-fold and 2-fold higher *LHCB1.2* transcript levels in two MORF2 overexpressors – similar to those seen in TPT14. In addition, it was not determined whether *LHCB1.2* levels were already higher in MORF2 overexpressors when grown on medium without inhibitor. During GUN1-dependent signaling, the GLK1/2 proteins receive the signals in the nucleus (Leister & Kleine, 2016; Martin et al., 2016) which are key regulators of *PhANG* transcript accumulation (Waters et al., 2009). It has previously been noted that light-dependent and chloroplast signaling pathways converge at some point (Leister et al., 2014; Martin et al., 2016; Ruckle et al., 2007), and recently BBX16 was identified as such a component (Veciana et al., 2022). *BBX16* was shown to be a direct target of GLK1 by ChIP-qPCR (Susila et al., 2023; Veciana et al., 2022) and indeed, BBX16 mediates the expression of a subset of GLK1-regulated *PhANG* genes under LIN conditions, but notably not that of *LHCB1.4* or *LHCB2.2* (Veciana et al., 2022). To detect further targets of GLK1, we chose a genome-wide approach (ChIP-Seq) and identified *BBX14*, *-15* and *BBX2*, *-4* and *-5* as additional direct targets of GLK1 (Figure 1; Table S1). They therefore fulfill the first criterion for membership of the GUN1/GLK-dependent biogenic signaling pathway. The second and third criteria could be transcript reduction in the presence of both NF and LIN and dependence on GUN1, respectively. Of the BBX members that fulfill criteria 2 and 3 (Figure S5), only BBX14, -15, and -16 also match criterion 1. Until now only one target (*CA1*) could be identified in BBX15 overexpression lines, and overexpression of BBX14 results in a "*gun*" phenotype similar to that seen in oeBBX16 lines (Figure 6), meaning that *LHCB1* transcript levels were not de-repressed in either BBX14 (our data) or in BBX16 overexpressors (Veciana et al., 2022). It should be emphasized that the original definition of a *gun* mutant was that of de-repression of *LHCB1* transcript levels despite seedlings were grown on NF (or LIN) (Ruckle et al., 2007; Susek et al., 1993). Although qPCR data might suggest a higher *LHCB1.2* expression in TPT14 compared to Col-0 when grown on NF (Figure 6b), it should be noted that *LHCB1.2* transcript levels were (i) variable from experiment to experiment, (ii) already slightly elevated on MS without inhibitor (Figure 6), (iii) well below those seen in the *gun1* mutant, (iv) clearly not higher in TPT14 when RNA-Seq data were plotted over the *LHCB1.2* gene. Our results should be viewed with caution because the one stable "overexpression" line that only showed elevated *CA1* levels had only 2.2-fold higher *BBX14* transcript levels than Col-0. But clearly, RT-qPCR results alone, especially when dealing with only 2-fold variation, do not appear to be completely reliable. Also, branching of the signaling pathway downstream of GLK1, as discussed by Veciana et al. (2022), might enable BBX14, BBX15 and BBX16 to regulate a subset of target genes, and additive functions may play a role here. For example, reduced GLK1 protein levels in damaged plastids are partially restored by MG132, a proteasome inhibitor, indicating that the ubiquitin-proteasome system participates in the degradation of GLK1 in response to plastid signals (Tokumaru et al., 2017), which adds yet another layer of complexity.

Whether only clade III BBX proteins have evolved to participate in retrograde signaling, or BBX factors from other clades are also involved remains to be determined.

The role of BBX proteins in acclimation to light stress

BBX14 transcript levels were notably decreased in plants exposed to HL (refer to Figure 7a,b). One hypothesis regarding the role of BBX14 in HL acclimation is that overexpression of BBX14 could aid plants in tolerating HL. In addition, it is possible that *bbx14* mutant lines would exhibit WT-like behavior, as BBX14 levels are readily down-regulated in these mutants. Nevertheless, under HL treatment, the "oeBBX14" plants behaved similarly to the WT, while the *bbx14* mutant plants suffered under HL. This suggests that BBX14 is beneficial for plant growth under HL. This finding can be elaborated like this: Alvarez-Fernandez et al. (2021) defined an accelerated HL acclimation phenotype as a significant enhancement of the operating efficiency of photosystem II (PSII; Y(II)). Because *BBX14* is co-regulated with *PhANG* transcripts under HL conditions (Garcia-Molina et al., 2020; Huang et al., 2019), this could in principle be achieved if higher BBX14 levels increased transcription levels of *PhANG* genes under HL, or a lack of BBX14 would result in less HL tolerant plants, which was indeed the case (Figure 7). Additionally, along with *BBX14*, transcriptional levels of all other clade III members and those of *BBX27* have been found to decrease under HL, while other *BBX* transcripts, including those of the clade V members *BBX29-BBX32*, were elevated (Garcia-Molina et al., 2020, Huang et al., 2019). A *bbx32* mutant displayed slightly higher Y(II) after 5 days of HL treatment, while plants overexpressing *BBX32* were impaired in acclimation to HL. Essentially, we have a situation of similar correlation between *BBX32* transcript and

© 2023 The Authors.

1365313x, 0, Downloaded from https://onlinelibrary.wiley.com/doi/10.1111/tpj.16597 by Cochrane Germany, Wiley Online Library on [08/03/2024]. See the Terms and Conditions (https://onlinelibrary.wiley.com/terms-and-conditions) on Wiley Online Library for rules of use; OA articles are governed by the applicable Creative Commons License

HL phenotype as observed for BBX14. But overexpression of BBX32 was already slightly detrimental under growth conditions with reduced amounts of several *PhANG* transcripts (Alvarez-Fernandez et al., 2021).

Overall, a picture is emerging in which BBX proteins have multi-layered functions in plant development, as well as important roles in responses to stress including the blockage of chloroplast development. However, our understanding of their specific functions is far from complete. Functional redundancies and feedback loops complicate their analysis, and further research will be required to reveal the precise regulatory networks and molecular mechanisms that mediate the signaling and its coordinated responses in nuclear gene regulation. In addition, we suggest continuing to use the old classification of *gun* mutants, that is, significant de-repression of *LHCB* (not only *CA1* or *RBCS*) transcript levels despite being grown on NF or LIN, to examine transcript levels not only by qPCR, and to always include a "classical," verified *gun* mutant as a control in all experiments.

EXPERIMENTAL PROCEDURES

Plant material and growth conditions

All the lines used were in the Col-0 background, and the mutants *bbx14-1* (SAIL_1221_D02; N878600) and *pifq* (N2107737) were obtained from the NASC and ABRC, respectively. The T-DNA insertion in *bbx14-1* was confirmed with the primers listed in Table S5 (see also Figure S1). The mutants *gun1-102* (Tadini et al., 2016), *gun4-2* (Peter & Grimm, 2009), and *glk1* (Waters et al., 2009) mutants have been described previously. The inducible overexpression lines (Coego et al., 2014) were obtained from the ABRC stock center.

Seeds were surface-sterilized in 10% bleach and 0.01% Triton-X-100 for 10 min, they were plated on sucrose-free agar (Sigma-Aldrich/Merck, Darmstadt, Germany) plates containing 0.5× MS medium followed by stratification at 4°C in dark for 3 days and growth at 22°C under 100 μmol photons m^{-2} sec^{-1} provided by white, fluorescent lamps. In the case of dark treatment, seeds were exposed to 2 h of white light (100 μmol photons m^{-2} sec^{-1}) after stratification, before allowing germination in the dark. For experiments involving lincomycin or norflurazon treatment, medium was supplemented with 0.5 mM lincomycin (Sigma-Aldrich) or 5 μM norflurazon (Sigma-Aldrich). Temperature (22°C/20°C during the day/night cycle) and relative humidity (60%) were strictly controlled under all conditions. For HL experiments, plants were pre-grown for 1 week in an LED chamber set to 80 μmol photons m^{-2} sec^{-1} (16-h light/8-h dark cycle) and then irradiance was increased to 1000 μmol photons m^{-2} sec^{-1} under strictly controlled temperature conditions.

In experiments performed with inducible overexpression lines, overexpression was induced by supplementing 0.5× MS medium with 2.5 μM β-estradiol or by spraying 4-day-old seedlings with a solution containing 20 μM β-estradiol (Sigma-Aldrich), 0.01% Silwet L-77 (Lehle seeds) and 0.2% DMSO. In case of experiments shown in Figure 6, induction was performed immediately after 3 days of dark treatment, followed by 2 h of dark incubation and subsequent growth for ≥16 h at 100 μmol photons m^{-2} sec^{-1} continuous white light.

Nucleic acid extraction

For DNA isolation, leaf tissue was homogenized in extraction buffer containing 200 mM Tris/HCl, pH 7.5, 25 mM NaCl, 20 mM EDTA, and 0.5% (w/v) SDS. After centrifugation, DNA was precipitated from the supernatant by adding isopropanol. After washing with 70% (v/v) ethanol, the DNA was dissolved in distilled water.

For RNA isolation, frozen tissue was ground in liquid nitrogen. Total RNA was extracted using Direct-zol™ RNA MiniPrep Plus columns (Zymo Research, Irvine, CA, USA) following the manufacturer's instructions. RNA quality and concentration and the A_{260}/A_{280} ratio were assessed by agarose gel electrophoresis and spectrophotometry. Isolated RNA was stored at −80°C prior to use.

cDNA synthesis and qRT-PCR analysis

First-strand cDNA synthesis and qRT-PCR were performed essentially as described previously (Wang et al., 2022), except that PCRs were carried out in the CFX Connect real-time system (Bio-Rad, Munich, Germany).

Generation of *BBX14* CRISPR and overexpression lines

The pHEE401-E vector, which provides an egg cell-specific promoter, was used to generate the *CRISPR-Cas* lines *bbx14-2* and *bbx14-3* (Wang et al., 2015). The specific guide RNA was designed using the web tool CHOPCHOP (http://chopchop.cbu.uib.no/) and cloned into pHEE401-E as described (Wang et al., 2015, 2022), and Col-0 plants were transformed with the construct via floral dipping using *Agrobacterium tumefaciens* GV3101 (Clough & Bent, 1998). Positive transformants were selected in the first generation (T1) on plates containing 0.5× MS medium supplemented with 50 μg ml^{-1} hygromycin and 1% (w/v) sucrose. To select for homozygous *bbx14* mutants, the *BBX14* gene was sequenced in the surviving plants using primers listed in Table S5.

For overexpression of BBX14 in Col-0, the *AT1G68520* coding region was amplified from cDNA by PCR (see Table S5 for primer information). The PCR product was then cloned with GATEWAY technology into both pB7FWG2 and pAUL1, thus generating fusions with the enhanced GFP-tag (eGFP) and HA-tag, respectively, which were expressed under the control of the Cauliflower Mosaic Virus *35S* promoter. Both constructs were introduced into Col-0 plants by floral dipping (Clough & Bent, 1998).

Generation of tagged GLK1 lines

To generate *Arabidopsis thaliana* Col-0 plants expressing GLK1-GFP from its endogenous promoter, the genomic locus of *GLK1* (including the 3867-bp promoter but excluding the stop codon) was amplified by PCR and subcloned into the pCR8/GW/TOPO TA cloning vector (Invitrogen, Carlsbad, CA, USA). The insert was transferred into the binary destination vector pMDC107 by LR reaction (pGLK1:gGLK1-GFP::pMDC107). Col-0 plants were transformed as described above.

Protein isolation and immunoblot analyses

Proteins were homogenized in 2× Laemmli sample buffer (120 mM Tris–HCl, pH 6.8, 4% SDS, 20% glycerol, 2.5% β-mercaptoethanol, 0.01% bromophenol blue), incubated for 10 min at 95°C, and centrifuged for 10 min. Proteins were fractionated in a 10% (w/v) SDS-polyacrylamide gel and transferred to polyvinylidene fluoride (PVDF) membranes (Millipore, Billerica, MA, USA)

© 2023 The Authors.

1365313x, 0, Downloaded from https://onlinelibrary.wiley.com/doi/10.1111/tpj.16597 by Cochrane Germany, Wiley Online Library on [08/03/2024]. See the Terms and Conditions (https://onlinelibrary.wiley.com/terms-and-conditions) on Wiley Online Library for rules of use; OA articles are governed by the applicable Creative Commons License

via semi-dry western transfer using Trans-Blot Turbo (Bio-Rad) in a buffer containing 25 mM Tris, 190 mM glycine, 0.1, and 20% methanol. Membranes were blocked with 5% (w/v) milk in TBS-T (10 mM Tris, pH 8.0, 150 mM NaCl, and 0.1% Tween 20), and probed with monoclonal anti-HA (G1546; Sigma-Aldrich) and anti-GFP (A6455; Life Technologies, Carlsbad, CA, USA) antibodies in 1:1000 and 1:5000 dilutions, respectively. Protein loading and transfer were verified by staining PVDF membranes with Coomassie brilliant blue R-250 dye. Signals were visualized via enhanced chemiluminescence Pierce™ ECL Western-Blotting substrate reagent (ThermoFisher Scientific, Waltham, MA, USA) using an ECL reader system (Fusion FX7; PeqLab, Darmstadt, Germany). Signals were and quantified using ImageJ software (http://rsbweb.nih.gov/ij).

Chlorophyll fluorescence analysis

In vivo chlorophyll *a* fluorescence of whole plants was recorded using an ImagingPAM chlorophyll fluorometer (Walz GmbH, Effeltrich, Germany) as described previously (Garcia-Molina et al., 2020).

Measurement of chlorophyll content

For chlorophyll extraction, approximately 100 mg of leaf tissue from 3-week-old plants was ground in liquid nitrogen in the presence of 80% (v/v) acetone. After removal of cell debris by centrifugation, chlorophyll absorption was measured spectrophotometrically. Pigment concentrations were calculated following Lichtenthaler (1987) and normalized to fresh weight.

Data analysis

Statistically significant differences in relative mRNA expression levels were tested by applying one-way ANOVA with Tukey's post-hoc HSD test (https://astatsa.com; version August 2021). The significance of differences in chlorophyll accumulation, hypocotyl lengths, F_v/F_m and Y(II) was tested by two-way ANOVA, followed by Tukey's multiple comparison test (as indicated in the Figure legends) using GraphPad Prism version 9.4.1 for Windows (GraphPad Software, www.graphpad.com). Samples were always compared with the respective wild-type (Col-0) sample within the same condition.

ChIP-seq sample preparation and data analysis

Seedlings (pGLK1:gGLK1-GFP in Col-0) were grown for 14 days under LD conditions (16 h light, 8 h dark) at 22°C. To assess whether different sugar and proteasome inhibitor treatments have an effect on GLK1-GFP stability and thus on the number and positions of identified DNA-binding sites, two growth conditions were applied: Half of the seedlings were grown on solid 0.5× MS medium supplemented with 3% sucrose until harvest at ZT8 on Day 14 ("untreated"). The second half of the seedlings were grown on solid 0.5× MS medium without sucrose. On Day 14 at ZT2, these seedlings were transferred to liquid 0.5 MS medium supplemented with 5% sucrose and 50 μM MG-132. They were then incubated for another 6 h in light until harvest at ZT8 ("treated"). 2.5–3 g of MG-132 treated versus untreated seedlings were harvested on ice and fixed as described (Kaufmann et al., 2010). Chromatin immunoprecipitation experiments and library preparation were performed using a GFP antibody (abcam 290) as described (Yan et al., 2018). Input DNA was processed in parallel for library preparation.

Fastq files were trimmed from adapter sequences using *Trimmomatic* v0.39 (Bolger et al., 2014). Reads were mapped to the Arabidopsis genome (TAIR10) using Bowtie2 v2.2.5 (Langmead & Salzberg, 2012) with default parameters. Only reads mapping to the nuclear chromosomes and with a mapping quality >40 were considered for further analysis. Peak calling was done with MACS2 v2.2.7.1 (Zhang et al., 2008) comparing IP versus control samples for each tissue independently with parameters: *-p=0.05*, *-c=220527*. Later, all the identified regions were merged in one file using *mergeBed* from the *BedTools* package (Quinlan & Hall, 2010). *FeatureCounts* (Liao et al., 2014) with parameters *-s 0* was used to obtain the number of mapped reads per region and ChIP-seq and control sample. *DEseq2* (Love et al., 2014) was used to detect regions with different number of reads between the IP samples and control. For each binding site, genes around the 1- or 3-kb binding regions are reported.

RNA-Seq and data analysis

Total RNA from plants was isolated using Trizol (Invitrogen) and purified using Direct-zol™ RNA MiniPrep Plus columns (Zymo Research, Irvine, CA, USA) according to the manufacturer's instructions, and RNA integrity and quality were assessed by an Agilent 2100 Bioanalyzer (Agilent, Santa Clara, CA, USA). Generation of RNA-Seq libraries and 150-bp paired-end sequencing was carried out on an Illumina HiSeq 2500 (Illumina, San Diego, CA, USA) or Novaseq6000 system by Novogene Biotech (Beijing, China) or Biomarker Technologies GmbH (Münster, Germany), respectively, using standard Illumina protocols. Three (Col and *bbx14* seedlings) or two (Col-0, *gun1*, and TPT14 seedlings grown on NF) independent biological replicates were used per genotype. RNA-Seq reads were analyzed on the Galaxy platform (Afgan et al., 2016) essentially as described before (Xu et al., 2019), except that reads were mapped with the gapped-read mapper RNA STAR (Dobin et al., 2013). In the TPT14 NF experiment, two-fold differentially expressed genes were identified without an adjusted *P*-value cut-off, because reads of one TPT14 NF replicate were of poor quality. This experiment was used to get a first impression of putative BBX14 targets during retrograde signaling and was therefore not repeated.

AUTHOR CONTRIBUTIONS

Conceptualization, formal analysis, and supervision: TK; investigation: VA, JS, JMM, and TK; generation of CRISPR lines, LW; help with HL experiments, CL; writing – original draft: TK with input from KK and VA; review and editing: DL and TK; funding acquisition: DL, KK and TK.

ACKNOWLEDGEMENTS

Funding was provided by the Deutsche Forschungsgemeinschaft to K.K., D.L., and T.K. (TRR175, projects C01 and C05). We thank Paul Hardy for critical comments on the manuscript, and Ramona Kandler for excellent technical assistance. Open Access funding enabled and organized by Projekt DEAL.

CONFLICT OF INTEREST

The authors declare no competing interests.

DATA AVAILABILITY STATEMENT

Sequencing data have been deposited in NCBI's Gene Expression Omnibus (Edgar et al., 2002) and are accessible under the GEO Series accession number GSE225039. Reads from experiments conducted by Habermann et al. (2020),

© 2023 The Authors.

1365313x, 0, Downloaded from https://onlinelibrary.wiley.com/doi/10.1111/tpj.16597 by Cochrane Germany, Wiley Online Library on [08/03/2024]. See the Terms and Conditions (https://onlinelibrary.wiley.com/terms-and-conditions) on Wiley Online Library for rules of use; OA articles are governed by the applicable Creative Commons License

Richter et al. (2020), Xu et al. (2020), and Zhao et al. (2019) were retrieved from the NCBI Sequence Read Archive (numbers PRJNA557616 and PRJNA432917, respectively) and Gene Expression Omnibus (numbers GSE104868 and GSE130337, respectively).

SUPPORTING INFORMATION

Additional Supporting Information may be found in the online version of this article.

Figure S1. Identification of *bbx14* mutant lines.

Figure S2. Investigation of putative *gun* phenotypes of seedlings containing altered levels of *BBX14*.

Figure S3. RNA-Seq of Col-0, TPT14 and *gun1* seedlings.

Figure S4. High light (HL) acclimation of *gun4-2* and "oeBBX14" plants.

Figure S5. Expression behavior of other *BBX* members under NF and LIN conditions.

Table S1. GLK1 ChIP-seq data analysis. Peaks with adjusted *P* values <0.05 are shown. Analysis was performed by DESeq 2 of both ChIP-seq samples versus input DNA.

Table S2. Genes whose transcript levels were significantly changed in 3-day-old etiolated *bbx14-1* seedlings compared to Col-0.

Table S3. Genes whose transcript levels were significantly changed in etiolated *bbx14-1* seedlings that were shifted to light for 1 day.

Table S4. Transcript level changes in gun1 and TPT14 seedlings (compared to Col-0) that were first grown for 3 days in darkness in the absence or presence of inhibitor (NF or LIN), then sprayed with the inducer, put back in the dark for 2 h, and finally transferred into the light for 16 h (100 μmol m^{-2} sec^{-1}).

Table S5. Primers used in this study.

REFERENCES

Afgan, E., Baker, D., van den Beek, M., Blankenberg, D., Bouvier, D., Cech, M. *et al.* (2016) The Galaxy platform for accessible, reproducible and collaborative biomedical analyses: 2016 update. *Nucleic Acids Research*, **44**, W3–W10.

Alonso, J.M., Stepanova, A.N., Leisse, T.J., Kim, C.J., Chen, H., Shinn, P. *et al.* (2003) Genome-wide insertional mutagenesis of *Arabidopsis thaliana*. *Science*, **301**, 653–657.

Alvarez-Fernandez, R., Penfold, C.A., Galvez-Valdivieso, G., Exposito-Rodriguez, M., Stallard, E.J., Bowden, L. *et al.* (2021) Time-series transcriptomics reveals a BBX32-directed control of acclimation to high light in mature Arabidopsis leaves. *The Plant Journal*, **107**, 1363–1386.

Bailey, T.L., Johnson, J., Grant, C.E. & Noble, W.S. (2015) The MEME suite. *Nucleic Acids Research*, **43**, W39–W49.

Bolger, A.M., Lohse, M. & Usadel, B. (2014) Trimmomatic: a flexible trimmer for Illumina sequence data. *Bioinformatics*, **30**, 2114–2120.

Buelbuel, S., Sakuraba, Y., Sedaghatmehr, M., Watanabe, M., Hoefgen, R., Balazadeh, S. *et al.* (2023) Arabidopsis BBX14 negatively regulates nitrogen starvation- and dark-induced leaf senescence. *The Plant Journal*, **116**, 251–268.

Cao, J., Liang, Y., Yan, T., Wang, X., Zhou, H., Chen, C. *et al.* (2022) The photomorphogenic repressors BBX28 and BBX29 integrate light and brassinosteroid signaling to inhibit seedling development in Arabidopsis. *Plant Cell*, **34**, 2266–2285.

Clough, S.J. & Bent, A.F. (1998) Floral dip: a simplified method for *Agrobacterium*-mediated transformation of *Arabidopsis thaliana*. *The Plant Journal*, **16**, 735–743.

Coego, A., Brizuela, E., Castillejo, P., Ruiz, S., Koncz, C., del Pozo, J.C. *et al.* (2014) The TRANSPLANTA collection of Arabidopsis lines: a resource for functional analysis of transcription factors based on their conditional overexpression. *The Plant Journal*, **77**, 944–953.

Datta, S., Hettiarachchi, C., Johansson, H. & Holm, M. (2007) SALT TOLERANCE HOMOLOG2, a B-box protein in Arabidopsis that activates transcription and positively regulates light-mediated development. *Plant Cell*, **19**, 3242–3255.

Datta, S., Hettiarachchi, G.H., Deng, X.W. & Holm, M. (2006) Arabidopsis CONSTANS-LIKE3 is a positive regulator of red light signaling and root growth. *Plant Cell*, **18**, 70–84.

Datta, S., Johansson, H., Hettiarachchi, C., Irigoyen, M.L., Desai, M., Rubio, V. *et al.* (2008) LZF1/SALT TOLERANCE HOMOLOG3, an Arabidopsis B-box protein involved in light-dependent development and gene expression, undergoes COP1-mediated ubiquitination. *Plant Cell*, **20**, 2324–2338.

Dobin, A., Davis, C.A., Schlesinger, F., Drenkow, J., Zaleski, C., Jha, S. *et al.* (2013) STAR: ultrafast universal RNA-seq aligner. *Bioinformatics*, **29**, 15–21.

Edgar, R., Domrachev, M. & Lash, A.E. (2002) Gene Expression Omnibus: NCBI gene expression and hybridization array data repository. *Nucleic Acids Research*, **30**, 207–210.

Fan, X.Y., Sun, Y., Cao, D.M., Bai, M.Y., Luo, X.M., Yang, H.J. *et al.* (2012) BZS1, a B-box protein, promotes photomorphogenesis downstream of both brassinosteroid and light signaling pathways. *Molecular Plant*, **5**, 591–600.

Franco-Zorrilla, J.M., Lopez-Vidriero, I., Carrasco, J.L., Godoy, M., Vera, P. & Solano, R. (2014) DNA-binding specificities of plant transcription factors and their potential to define target genes. *Proceedings of the National Academy of Sciences of the United States of America*, **111**, 2367–2372.

Fu, L.Y., Zhu, T., Zhou, X., Yu, R., He, Z., Zhang, P. *et al.* (2022) ChIP-Hub provides an integrative platform for exploring plant regulome. *Nature Communications*, **13**, 3413.

Gangappa, S.N. & Botto, J.F. (2014) The BBX family of plant transcription factors. *Trends in Plant Science*, **19**, 460–470.

Garcia-Molina, A., Kleine, T., Schneider, K., Muhlhaus, T., Lehmann, M. & Leister, D. (2020) Translational components contribute to acclimation responses to high light, heat, and cold in Arabidopsis. *iScience*, **23**, 101331.

Habermann, K., Tiwari, B., Krantz, M., Adler, S.O., Klipp, E., Arif, M.A. *et al.* (2020) Identification of small non-coding RNAs responsive to GUN1 and GUN5 related retrograde signals in *Arabidopsis thaliana*. *The Plant Journal*, **104**, 138–155.

Han, X., Huang, X. & Deng, X.W. (2020) The photomorphogenic central repressor COP1: conservation and functional diversification during evolution. *Plant Communications*, **1**, 100044.

Heng, Y., Lin, F., Jiang, Y., Ding, M., Yan, T., Lan, H. *et al.* (2019) B-box containing proteins BBX30 and BBX31, acting downstream of HY5, negatively regulate photomorphogenesis in Arabidopsis. *Plant Physiology*, **180**, 497–508.

Holtan, H.E., Bandong, S., Marion, C.M., Adam, L., Tiwari, S., Shen, Y. *et al.* (2011) BBX32, an Arabidopsis B-box protein, functions in light signaling by suppressing HY5-regulated gene expression and interacting with STH2/BBX21. *Plant Physiology*, **156**, 2109–2123.

Huang, J., Zhao, X. & Chory, J. (2019) The Arabidopsis transcriptome responds specifically and dynamically to high light stress. *Cell Reports*, **29**, 4186–4199.e3.

Jan, M., Liu, Z., Rochaix, J.-D. & Sun, X. (2022) Retrograde and anterograde signaling in the crosstalk between chloroplast and nucleus. *Frontiers in Plant Science*, **13**, 980237.

Kaufmann, K., Muino, J.M., Osteras, M., Farinelli, L., Krajewski, P. & Angenent, G.C. (2010) Chromatin immunoprecipitation (ChIP) of plant transcription factors followed by sequencing (ChIP-SEQ) or hybridization to whole genome arrays (ChIP-CHIP). *Nature Protocols*, **5**, 457–472.

Khanna, R., Kronmiller, B., Maszle, D.R., Coupland, G., Holm, M., Mizuno, T. *et al.* (2009) The Arabidopsis B-box zinc finger family. *Plant Cell*, **21**, 3416–3420.

Khanna, R., Shen, Y., Toledo-Ortiz, G., Kikis, E.A., Johannesson, H., Hwang, Y.S. *et al.* (2006) Functional profiling reveals that only a small number of phytochrome-regulated early-response genes in Arabidopsis are necessary for optimal deetiolation. *Plant Cell*, **18**, 2157–2171.

Kleine, T., Kindgren, P., Benedict, C., Hendrickson, L. & Strand, A. (2007) Genome-wide gene expression analysis reveals a critical role for CRYPTOCHROME1 in the response of Arabidopsis to high irradiance. *Plant Physiology*, **144**, 1391–1406.

© 2023 The Authors.

1365313x, 0, Downloaded from https://onlinelibrary.wiley.com/doi/10.1111/tpj.16597 by Cochrane Germany, Wiley Online Library on [08/03/2024]. See the Terms and Conditions (https://onlinelibrary.wiley.com/terms-and-conditions) on Wiley Online Library for rules of use; OA articles are governed by the applicable Creative Commons License

Kleine, T. & **Leister, D.** (2016) Retrograde signaling: organelles go networking. *Biochimica et Biophysica Acta*, **1857**, 1313–1325.
Kobayashi, K., **Obayashi, T.** & **Masuda, T.** (2012) Role of the G-box element in regulation of chlorophyll biosynthesis in Arabidopsis roots. *Plant Signaling & Behavior*, **7**, 922–926.
Koussevitzky, S., **Nott, A.**, **Mockler, T.C.**, **Hong, F.**, **Sachetto-Martins, G.**, **Surpin, M.** ***et al.*** (2007) Signals from chloroplasts converge to regulate nuclear gene expression. *Science*, **316**, 715–719.
Kumagai, T., **Ito, S.**, **Nakamichi, N.**, **Niwa, Y.**, **Murakami, M.**, **Yamashino, T.** ***et al.*** (2008) The common function of a novel subfamily of B-box zinc finger proteins with reference to circadian-associated events in *Arabidopsis thaliana*. *Bioscience, Biotechnology, and Biochemistry*, **72**, 1539–1549.
Langmead, B. & **Salzberg, S.L.** (2012) Fast gapped-read alignment with Bowtie 2. *Nature Methods*, **9**, 357–359.
Leister, D. & **Kleine, T.** (2016) Definition of a core module for the nuclear retrograde response to altered organellar gene expression identifies GLK overexpressors as gun mutants. *Physiologia Plantarum*, **157**, 297–309.
Leister, D., **Romani, I.**, **Mittermayr, L.**, **Paieri, F.**, **Fenino, E.** & **Kleine, T.** (2014) Identification of target genes and transcription factors implicated in translation-dependent retrograde signaling in Arabidopsis. *Molecular Plant*, **7**, 1228–1247.
Liao, Y., **Smyth, G.K.** & **Shi, W.** (2014) featureCounts: an efficient general purpose program for assigning sequence reads to genomic features. *Bioinformatics*, **30**, 923–930.
Lichtenthaler, H.K. (1987) Chlorophylls and carotenoids–pigments of photosynthetic biomembranes. *Methods in Enzymology*, **148**, 350–382. https://doi.org/10.1016/0076-6879(87)48036-1.
Liebers, M., **Cozzi, C.**, **Uecker, F.**, **Chambon, L.**, **Blanvillain, R.** & **Pfannschmidt, T.** (2022) Biogenic signals from plastids and their role in chloroplast development. *Journal of Experimental Botany*, **73**, 7105–7125.
Love, M.I., **Huber, W.** & **Anders, S.** (2014) Moderated estimation of fold change and dispersion for RNA-seq data with DESeq2. *Genome Biology*, **15**, 550.
Martin, G., **Leivar, P.**, **Ludevid, D.**, **Tepperman, J.M.**, **Quail, P.H.** & **Monte, E.** (2016) Phytochrome and retrograde signalling pathways converge to antagonistically regulate a light-induced transcriptional network. *Nature Communications*, **7**, 11431.
Oelmuller, R., **Levitan, I.**, **Bergfeld, R.**, **Rajasekhar, V.K.** & **Mohr, H.** (1986) Expression of nuclear genes as affected by treatments acting on the plastids. *Planta*, **168**, 482–492.
Peter, E. & **Grimm, B.** (2009) GUN4 is required for posttranslational control of plant tetrapyrrole biosynthesis. *Molecular Plant*, **2**, 1198–1210.
Podolec, R. & **Ulm, R.** (2018) Photoreceptor-mediated regulation of the COP1/-SPA E3 ubiquitin ligase. *Current Opinion in Plant Biology*, **45**, 18–25.
Pogson, B.J., **Woo, N.S.**, **Forster, B.** & **Small, I.D.** (2008) Plastid signalling to the nucleus and beyond. *Trends in Plant Science*, **13**, 602–609.
Putterill, J., **Robson, F.**, **Lee, K.**, **Simon, R.** & **Coupland, G.** (1995) The CONSTANS gene of Arabidopsis promotes flowering and encodes a protein showing similarities to zinc finger transcription factors. *Cell*, **80**, 847–857.
Quinlan, A.R. & **Hall, I.M.** (2010) BEDTools: a flexible suite of utilities for comparing genomic features. *Bioinformatics*, **26**, 841–842.
Richter, A.S., **Nagele, T.**, **Grimm, B.**, **Kaufmann, K.**, **Schroda, M.**, **Leister, D.** ***et al.*** (2023) Retrograde signaling in plants: a critical review focusing on the GUN pathway and beyond. *Plant Communications*, **4**, 100511.
Richter, A.S., **Tohge, T.**, **Fernie, A.R.** & **Grimm, B.** (2020) The genomes uncoupled-dependent signalling pathway coordinates plastid biogenesis with the synthesis of anthocyanins. *Philosophical Transactions of the Royal Society of London. Series B, Biological Sciences*, **375**, 20190403.
Ruckle, M.E., **DeMarco, S.M.** & **Larkin, R.M.** (2007) Plastid signals remodel light signaling networks and are essential for efficient chloroplast biogenesis in Arabidopsis. *Plant Cell*, **19**, 3944–3960.
Sherman, B.T., **Hao, M.**, **Qiu, J.**, **Jiao, X.**, **Baseler, M.W.**, **Lane, H.C.** ***et al.*** (2022) DAVID: a web server for functional enrichment analysis and functional annotation of gene lists (2021 update). *Nucleic Acids Research*, **50**, W216–W221.
Song, Z., **Yan, T.**, **Liu, J.**, **Bian, Y.**, **Heng, Y.**, **Lin, F.** ***et al.*** (2020) BBX28/BBX29, HY5 and BBX30/31 form a feedback loop to fine-tune photomorphogenic development. *The Plant Journal*, **104**, 377–390.
Susek, R.E., **Ausubel, F.M.** & **Chory, J.** (1993) Signal transduction mutants of Arabidopsis uncouple nuclear CAB and RBCS gene expression from chloroplast development. *Cell*, **74**, 787–799.
Susila, H., **Nasim, Z.**, **Gawarecka, K.**, **Jung, J.Y.**, **Jin, S.**, **Youn, G.** ***et al.*** (2023) Chloroplasts prevent precocious flowering through a GOLDEN2-LIKE-B-BOX DOMAIN PROTEIN module. *Plant Communications*, **4**, 100515.
Tadini, L., **Pesaresi, P.**, **Kleine, T.**, **Rossi, F.**, **Guljamow, A.**, **Sommer, F.** ***et al.*** (2016) GUN1 controls accumulation of the plastid ribosomal protein S1 at the protein level and interacts with proteins involved in plastid protein homeostasis. *Plant Physiology*, **170**, 1817–1830.
Talar, U. & **Kielbowicz-Matuk, A.** (2021) Beyond Arabidopsis: BBX regulators in crop plants. *International Journal of Molecular Sciences*, **22**, 2906.
Tokumaru, M., **Adachi, F.**, **Toda, M.**, **Ito-Inaba, Y.**, **Yazu, F.**, **Hirosawa, Y.** ***et al.*** (2017) Ubiquitin-proteasome dependent regulation of the GOLDEN2-LIKE 1 transcription factor in response to plastid signals. *Plant Physiology*, **173**, 524–535.
Vaishak, K.P., **Yadukrishnan, P.**, **Bakshi, S.**, **Kushwaha, A.K.**, **Ramachandran, H.**, **Job, N.** ***et al.*** (2019) The B-box bridge between light and hormones in plants. *Journal of Photochemistry and Photobiology. B*, **191**, 164–174.
Veciana, N., **Martin, G.**, **Leivar, P.** & **Monte, E.** (2022) BBX16 mediates the repression of seedling photomorphogenesis downstream of the GUN1/GLK1 module during retrograde signalling. *The New Phytologist*, **234**, 93–106.
Von Arnim, A. & **Deng, X.W.** (1996) Light control of seedling development. *Annual Review of Plant Physiology and Plant Molecular Biology*, **47**, 215–243.
Wang, H., **Zhang, Z.**, **Li, H.**, **Zhao, X.**, **Liu, X.**, **Ortiz, M.** ***et al.*** (2013) CONSTANS-LIKE 7 regulates branching and shade avoidance response in Arabidopsis. *Journal of Experimental Botany*, **64**, 1017–1024.
Wang, L., **Xu, D.**, **Scharf, K.**, **Frank, W.**, **Leister, D.** & **Kleine, T.** (2022) The RNA-binding protein RBP45D of Arabidopsis promotes transgene silencing and flowering time. *The Plant Journal*, **109**, 1397–1415.
Wang, Z.P., **Xing, H.L.**, **Dong, L.**, **Zhang, H.Y.**, **Han, C.Y.**, **Wang, X.C.** ***et al.*** (2015) Egg cell-specific promoter-controlled CRISPR/Cas9 efficiently generates homozygous mutants for multiple target genes in Arabidopsis in a single generation. *Genome Biology*, **16**, 144.
Waters, M.T., **Wang, P.**, **Korkaric, M.**, **Capper, R.G.**, **Saunders, N.J.** & **Langdale, J.A.** (2009) GLK transcription factors coordinate expression of the photosynthetic apparatus in Arabidopsis. *Plant Cell*, **21**, 1109–1128.
Winter, D., **Vinegar, B.**, **Nahal, H.**, **Ammar, R.**, **Wilson, G.V.** & **Provart, N.J.** (2007) An "Electronic Fluorescent Pictograph" browser for exploring and analyzing large-scale biological data sets. *PLoS One*, **2**, e718.
Xu, D. (2020) COP1 and BBXs-HY5-mediated light signal transduction in plants. *The New Phytologist*, **228**, 1748–1753.
Xu, D., **Dhiman, R.**, **Garibay, A.**, **Mock, H.P.**, **Leister, D.** & **Kleine, T.** (2020) Cellulose defects in the Arabidopsis secondary cell wall promote early chloroplast development. *The Plant Journal*, **101**, 156–170.
Xu, D., **Marino, G.**, **Klingl, A.**, **Enderle, B.**, **Monte, E.**, **Kurth, J.** ***et al.*** (2019) Extrachloroplastic PP7L functions in chloroplast development and abiotic stress tolerance. *Plant Physiology*, **180**, 323–341.
Xu, X., **Xu, J.**, **Yuan, C.**, **Chen, Q.**, **Liu, Q.**, **Wang, X.** ***et al.*** (2022) BBX17 interacts with CO and negatively regulates flowering time in *Arabidopsis thaliana*. *Plant & Cell Physiology*, **63**, 401–409.
Yan, W., **Chen, D.**, **Smaczniak, C.**, **Engelhorn, J.**, **Liu, H.**, **Yang, W.** ***et al.*** (2018) Dynamic and spatial restriction of Polycomb activity by plant histone demethylases. *Nature Plants*, **4**, 681–689.
Yuan, L., **Yu, Y.**, **Liu, M.**, **Song, Y.**, **Li, H.**, **Sun, J.** ***et al.*** (2021) BBX19 fine-tunes the circadian rhythm by interacting with PSEUDO-RESPONSE REGULATOR proteins to facilitate their repressive effect on morning-phased clock genes. *Plant Cell*, **33**, 2602–2617.
Zhang, X., **Huai, J.**, **Shang, F.**, **Xu, G.**, **Tang, W.**, **Jing, Y.** ***et al.*** (2017) A PIF1/PIF3-HY5-BBX23 transcription factor cascade affects photomorphogenesis. *Plant Physiology*, **174**, 2487–2500.
Zhang, Y., **Liu, T.**, **Meyer, C.A.**, **Eeckhoute, J.**, **Johnson, D.S.**, **Bernstein, B.E.** ***et al.*** (2008) Model-based analysis of ChIP-Seq (MACS). *Genome Biology*, **9**, R137.
Zhang, Z., **Ji, R.**, **Li, H.**, **Zhao, T.**, **Liu, J.**, **Lin, C.** ***et al.*** (2014) CONSTANS-LIKE 7 (COL7) is involved in phytochrome B (phyB)-mediated light-quality regulation of auxin homeostasis. *Molecular Plant*, **7**, 1429–1440.
Zhao, X., **Huang, J.** & **Chory, J.** (2019) GUN1 interacts with MORF2 to regulate plastid RNA editing during retrograde signaling. *Proceedings of the National Academy of Sciences of the United States of America*, **116**, 10162–10167.

© 2023 The Authors.

1365313x, 0, Downloaded from https://onlinelibrary.wiley.com/doi/10.1111/tpj.16597 by Cochrane Germany, Wiley Online Library on [08/03/2024]. See the Terms and Conditions (https://onlinelibrary.wiley.com/terms-and-conditions) on Wiley Online Library for rules of use; OA articles are governed by the applicable Creative Commons License